

ornl

ORNL/Sub/91-SH641/1

**OAK RIDGE
NATIONAL
LABORATORY**

MARTIN MARIETTA

**ENHANCED ABSORPTION CYCLE
COMPUTER MODEL**

**G. Grossman and M. Wilk
Faculty of Mechanical Engineering
Technion—Israel Institute of Technology
Haifa 32000, Israel**

Final Report

**Prepared for the
OAK RIDGE NATIONAL LABORATORY
Oak Ridge, Tennessee 37831
managed by
MARTIN MARIETTA ENERGY SYSTEMS, INC.
for the
U.S. DEPARTMENT OF ENERGY
under Contract No. DE-AC05-84OR21400**

**MANAGED BY
MARTIN MARIETTA ENERGY SYSTEMS, INC.
FOR THE UNITED STATES
DEPARTMENT OF ENERGY**

ENHANCED ABSORPTION CYCLE COMPUTER MODEL

G. Grossman and M. Wilk
Faculty of Mechanical Engineering
Technion—Israel Institute of Technology
Haifa 32000, Israel
Subcontract 19X-SH641V

DATE PUBLISHED: SEPTEMBER 1993

Prepared for the
OAK RIDGE NATIONAL LABORATORY
Oak Ridge, Tennessee 37831
managed by
MARTIN MARIETTA ENERGY SYSTEMS, INC.
for the
U.S. DEPARTMENT OF ENERGY
under Contract No. DE-AC05-84OR21400

CONTENTS

	<u>Page</u>
LIST OF FIGURES	v
ABSTRACT	vii
NOMENCLATURE, ACRONYMS, AND SUBSCRIPTS	ix
1. INTRODUCTION.....	1
2. STRUCTURE OF THE COMPUTER MODEL.....	2
3. UNIT SUBROUTINES AND GOVERNING EQUATIONS	6
4. MATERIAL PROPERTIES.....	11
5. CONSTRUCTION OF MATHEMATICAL MODEL.....	12
6. ALGORITHM OF SOLUTION.....	14
7. SIMULATION RESULTS	17
8. CONCLUSION.....	25
9. REFERENCES	26
ACKNOWLEDGMENTS.....	28
APPENDIX A. RESULTS OF CALCULATIONS.....	29
APPENDIX B. USERS' MANUAL	37

LIST OF FIGURES

<u>Figure</u>		<u>Page</u>
1	Structure of the computer code	3
2	Schematic description of individual components forming absorption systems.....	7
3	Coefficient of performance (COP) for double-effect, series flow system (solid lines), and single-effect system (broken lines) as functions of operating temperatures. Carnot COP for the same operating conditions is given for comparison	18
4	Schematic description of triple-effect lithium bromide-water systems. (a) series connection, (b) parallel connection	20
5	Schematic description of solar powered open absorption systems. (a) direct regeneration, (b) indirect regeneration.....	21
6	Schematic description of single-effect ammonia-water system	23
7	Schematic description of ammonia-water generator-absorber heat exchange (GAX) cycle	24

ABSTRACT

A computer code has been developed for simulation of absorption systems at steady state in a flexible and modular form, making it possible to investigate various cycle configurations with different working fluids. The code is based on unit subroutines containing the governing equations for the system's components and property subroutines containing thermodynamic properties of the working fluids. The components are linked together by a main program according to the user's specifications to form the complete system. Once all the equations have been established, a mathematical solver routine is employed to solve them simultaneously.

The user-oriented code requires a relatively simple input, which contains the given operating conditions and the working fluid at each state point. The user conveys to the computer an image of his cycle by specifying the different subunits and their interconnections. Based on this information, the program calculates the temperature, flow rate, concentration, pressure, and vapor fraction at each state point in the system, and the heat duty at each unit, from which the coefficient of performance (COP) may be determined.

This report describes the code and its operation, including improvements introduced into the present version. Particular attention has been devoted to the mathematical portion of the code to enhance its capability to converge with large and complex cycles. Simulation results are described for LiBr-H₂O triple-effect cycles, LiCl-H₂O solar-powered open absorption cycles, and NH₃-H₂O single-effect and generator-absorber heat exchange (GAX) cycles.

NOMENCLATURE, ACRONYMS, AND SUBSCRIPTS

A	heat transfer area (ft ² or m ²)
C	absorbent/absorbate concentration (weight %)
CAT	closest approach temperature (°F or °C)
CH ₃ OH	methyl alcohol (methanol)
COP	coefficient of performance
Δ	step-length restrictor, defining "trust region" (dimensionless)
DEV	extent of deviation from equilibrium state (°F or °C)
δ _k	current step (dimensionless)
δ _n	Newton step, Eq. (18)
DOE	U.S. Department of Energy
DR	direct regeneration
ε	residual of function (dimensionless)
EFF	heat transfer effectiveness (dimensionless)
F	mass flow rate (lb/min or kg/sec)
f	sum of squares of the functions, Eq. (19) (dimensionless)
g	steepest-descent step, Eq. (20) (dimensionless)
GAX	generator-absorber heat exchange
h	specific enthalpy (Btu/lb or kJ/kg)
IR	indirect regeneration
J(X)	Jacobian matrix of the system of equations
LiBr	lithium bromide
LiCl	lithium chloride
LMTD	logarithmic mean temperature difference (°F or °C)
m	number of equations
n	number of unknowns
NH ₃	ammonia
ORNL	Oak Ridge National Laboratory
P	pressure (psia or kPa)
PTX	Vapor pressure-temperature-concentration
Q	heat transfer rate (Btu/min or kW)
R	symbol for function, Eq. (7) (dimensionless)
R&D	research and development
T	temperature (°F or °C)
U	overall heat transfer coefficient [Btu/(ft ² · F · min) or kW/m ² · °C]

UA	overall heat transfer coefficient times area (Btu/F·min. or kW/ °C)
w	vapor mass fraction (dimensionless)
X	symbol for unknown variable (dimensionless)
ZnBr ₂	zinc bromide

Subscripts

E	=	equilibrium
i, j, or numerical	=	state point index
k	=	number of current iteration
L	=	liquid
Pr	=	projection
V	=	vapor

1. INTRODUCTION

Absorption heat pumps, once dominant in the cooling industry, have received renewed and increasing attention in the past two decades. The rising cost of electricity has made the particular features of this heat-powered cycle attractive for both residential and industrial applications. Solar-powered absorption chillers, gas-fired domestic heat pumps, and waste-heat-powered industrial temperature boosters are a few of the applications recently subjected to intensive research and development (R&D). Some of these developments have matured into commercial products that are competing successfully in the market with their electric-powered counterparts. The absorption heat pump research community has begun to search for both advanced cycles in various multistage configurations and new working fluid combinations with potential for enhanced performance and reliability.

The development of working absorption systems has created a need for reliable and effective system simulations. Several system-specific computer models have been developed [1–5] that have proven to be very valuable tools for R&D and for design optimization. Some of the models were validated against experimental data with good agreement. However, system-specific models are quite restricted. All of the models mentioned were limited to the particular system for which they were created; their structure did not allow easy modification for modeling other systems. For that to be done, major parts of the code, particularly the iterative sequence, required rewriting by the user for each new cycle.

The objective of the present work has been to develop a modular computer code capable of simulating absorption systems in different cycle configurations and with different working fluids. The usefulness of such a code has become apparent during repeated attempts under absorption research programs to evaluate new ideas for absorption cycles and working substances and to compare them with existing ones. Earlier publications [6–8] described the modular approach taken to achieve this flexibility without the need for the user to worry about the iterative scheme or do any programming. Simulation capabilities of the code in its earlier versions were also described in refs. [6–8]. The main shortcoming of these versions has been their failure to achieve convergence for complex systems.

This report describes a further improved version of the code with considerably extended, user-oriented simulation capability and applicability. Particular effort has been devoted to the mathematical portion of the code to enhance its convergence capability for large and complex cycles. As will be shown, the code in its present form may be used not only for evaluating new cycles and working fluids, but also to investigate a system's behavior in off-design conditions, to analyze experimental data, and to perform preliminary design optimization.

2. STRUCTURE OF THE COMPUTER MODEL

Developing a flexible and user-oriented simulation code has led to several basic requirements with respect to its structure. First, to enable the user to specify different cycle configurations, different working fluids, and obviously different unit sizes and operating conditions, the code had to be modular in nature. Second, to keep the input requirements simple and the application straightforward, the code had to contain, as an integral part, all the equations and algorithms required for the solution. The decision was made early on to eliminate the need for the user to write parts of the code specific to the cycle, in the form of external subroutines or otherwise, as is often done in sequential flowsheeting simulators. This is the case because in a closed cycle containing several loops, defining a stable sequence of iteration can constitute a major difficulty for the user.

The structure of the code is based on the following logic: recognizing that each absorption system consists of a number of standard components (e.g., absorber, evaporator, desorber, condenser, etc.), and that each of those components can employ a variety of working fluids, the code is built upon unit subroutines and property subroutines in separate modules. Each basic component is simulated by a unit subroutine that provides a mathematical expression of the physics of that component. The unit subroutine contains all the physical equations required to fully describe its behavior, such as energy balance, conservation of mass for each material species, heat and mass transfer, and thermodynamic equilibrium. When activated, the unit subroutine calls upon the property subroutines, contained in a property data base, for the thermodynamic properties of the working fluids. This separation between the unit subroutines and property subroutines provides the flexibility for each unit to operate with different working fluids. The main program calls the unit subroutines and links the components together in a form corresponding to the user's specification of the cycle. Each call to a unit subroutine is equivalent to collecting all the equations associated with it without attempting to solve them as yet. When the calls to all the unit subroutines have been completed, all the equations have been established, and a mathematical solver routine is employed to solve the set of nonlinear equations simultaneously. During the solution process, the solver calls the unit subroutines to calculate the residual values of the equations for definite values of the variables.

Figure 1 is a schematic description of the program architecture. With input, the user conveys to the program an "image" of the cycle to be simulated: the number and types of units contained in it, their interconnections, and their size (or transfer characteristics, where applicable). The input must also specify the working fluids and must contain the values of the parameters set by the user (e.g., temperatures, flow rates, etc.) at specific state points. The main program interprets the input and creates a variable vector containing all the independent unknown quantities. It then

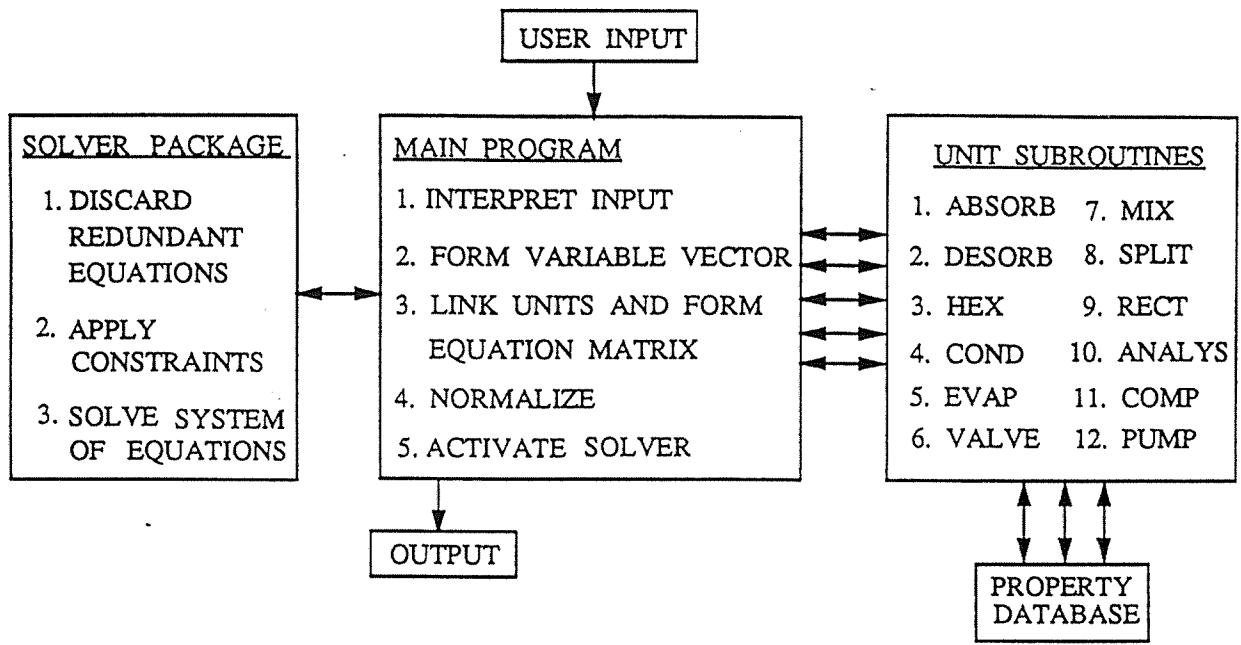


Fig. 1. Structure of the computer code.

calls the unit subroutines, thereby establishing the system's governing equations. The unit subroutines refer to the property data base as illustrated. All the equations and variables are normalized and brought to the same order of magnitude. The solver package is then activated, and the values of the unknowns are calculated to a user-specified accuracy. Because the set of nonlinear equations may have more than one mathematical solution, the physical validity of the solution is ensured by applying linear constraints on the variables, which define a feasible region. The output contains the temperature, enthalpy, flow rate, concentration, pressure, and vapor fraction at each of the cycle's state points, as well as the heat duty and transfer characteristics of each unit.

Unlike most process simulators and flowsheeting programs commonly used by the chemical industry, the present program does not require the user to do any programming. Further, because all the governing equations are solved simultaneously, the user does not have to specify an iterative sequence by which the program is to proceed through a cycle, which eliminates the worry about the order of variables and parameters. To prepare an input, the user first draws a schematic diagram depicting the cycle to be simulated in terms of the twelve basic units recognizable by the code (Fig. 1). A detailed description of these units and their governing equations will follow. The diagram must display schematically the system's breakdown into the basic units and their interconnections. The user must label each state point and each unit, in an arbitrary order. The input consists of the following three parts:

1. General Information—containing a user-supplied problem title, scaling parameters for normalization, limits on the number of iterations, and convergence criteria. Default options are available for all of the above. The code can operate either in Standard International or British units, as indicated by a proper flag. The total numbers of units and state points are specified.
2. Unit Input—for each of the units in the cycle, showing the unit number in the diagram, its type, its heat and mass transfer characteristics, and a list of its state point numbers in the schematic diagram in an order corresponding to that of the unit subroutine. Heat transfer characteristics of a unit may be specified by one of four methods. The user can supply either the UA (overall heat transfer coefficient times area), the EFF (effectiveness), the CAT (closest approach temperature), or the LMTD (logarithmic mean temperature difference). Mass transfer characteristics of a unit are specified by a temperature deviation (DEV) from equilibrium at the outlet.
3. State Point Input—for each of the state points in the cycle, showing the state point number, a code for the working fluid in it, and five pairs of numbers for the temperature, flow rate, concentration, vapor pressure, and vapor fraction in that state point. Each pair of numbers consists of an integer index and a real value. The former can

be either zero or non-zero, indicating a fixed or variable quantity, respectively. The latter gives a fixed value or an initial guess for the quantity in question.

In summary, this form of user input completely conveys to the program the necessary information about a given cycle, without the need for any programming. In the unit input, the program is told which units are contained in the cycle, what their heat and mass transfer characteristics are, and how they are interconnected. In the state point input, the program is told the fixed and variable parameters of the problem, which working fluids are used, and where they are used. Additional details have been included in the users' manual (see Appendix B).

The main program is the coordinator among the different modules shown in Fig. 1. The principal tasks performed by the main program are interpreting the user input and constructing a mathematical model of the cycle. The latter task includes forming a vector of normalized variables, linking the units and forming the system of equations and constraints, testing for and eliminating redundant equations, and (if necessary) forming the pattern of the Jacobian. Then the solver is activated. As illustrated in Fig. 1, the main program calls the unit subroutines and the solver package, when required.

By scanning through the State Point Input, the main program is able to identify the variable quantities by their non-zero flag. The physical variables are normalized by division with the proper scaling parameters, which are taken from the General Information section of the Input. The variable vector can contain unknown temperatures, flow rates, concentrations, pressures, and vapor fractions. Other unknown properties such as enthalpy are treated as dependent variables and are calculated at each iteration from the current values of the properties in the variable vector. Calling the unit subroutines in the order given in the Unit Input enables the main program to collect the equations associated with each, and to substitute in them the appropriate variables and fixed quantities as mandated by the unit's interconnections. The equations are counted, and each is assigned a number. During the solution process, the residuals of the equations are calculated at successive iterations. The equations are normalized using the scaling parameters.

Before beginning to solve, the program displays (at the user's request) the total number of equations and unknowns. Usually, the former exceeds the latter because calls to unit subroutines sometimes generate redundant equations originating from essentially identical mass balances at different units. The redundant equations are eliminated automatically by the program. When all the unknown variables have been computed to the desired accuracy, the main program converts them back from the dimensionless values to physical values.

Each of the program's parts mentioned in the preceding section (and illustrated in Fig. 1) has been described and elaborated upon in ref. [7]. The following chapters will discuss certain modules of the code where significant changes have been introduced relative to earlier versions.

3. UNIT SUBROUTINES AND GOVERNING EQUATIONS

Figure 2 illustrates the twelve standard units recognizable by the code, with their respective state points. The units, with their identity code given in parentheses, are as follows: absorber (1), desorber (2), heat exchanger (3), condenser (4), evaporator (5), valve (6), mixer (7), splitter (8), rectifier (9), analyzer (10), compressor (11), and pump (12). These units were found sufficient to create most absorption cycles of interest. Each unit is treated as a black box, with its own inputs and outputs, that can be connected to other components. The governing equations take the unit as a whole and are formed from some or all of the following physical laws:

a. Conservation of total mass:

$$\sum_i F_i = 0 . \quad (1)$$

b. Conservation of mass for each material species (absorbent-absorbate):

$$\sum_i (F_i C_i) = 0 . \quad (2)$$

c. Energy balance:

$$\sum_i (F_i h_i) = 0 . \quad (3)$$

d. Heat transfer, expressed in either of the following four forms:

$$Q_{UNIT} - UA * \overline{LMTD} = 0 , \quad (4a)$$

$$EFF - \overline{EFF} = 0 , \quad (4b)$$

$$CAT - \overline{CAT} = 0 , \text{ or} \quad (4c)$$

$$LMTD - \overline{LMTD} = 0 , \quad (4d)$$

where EFF, CAT, and LMTD are user-supplied values of heat transfer effectiveness, closest approach temperature, and logarithmic mean temperature difference, respectively,

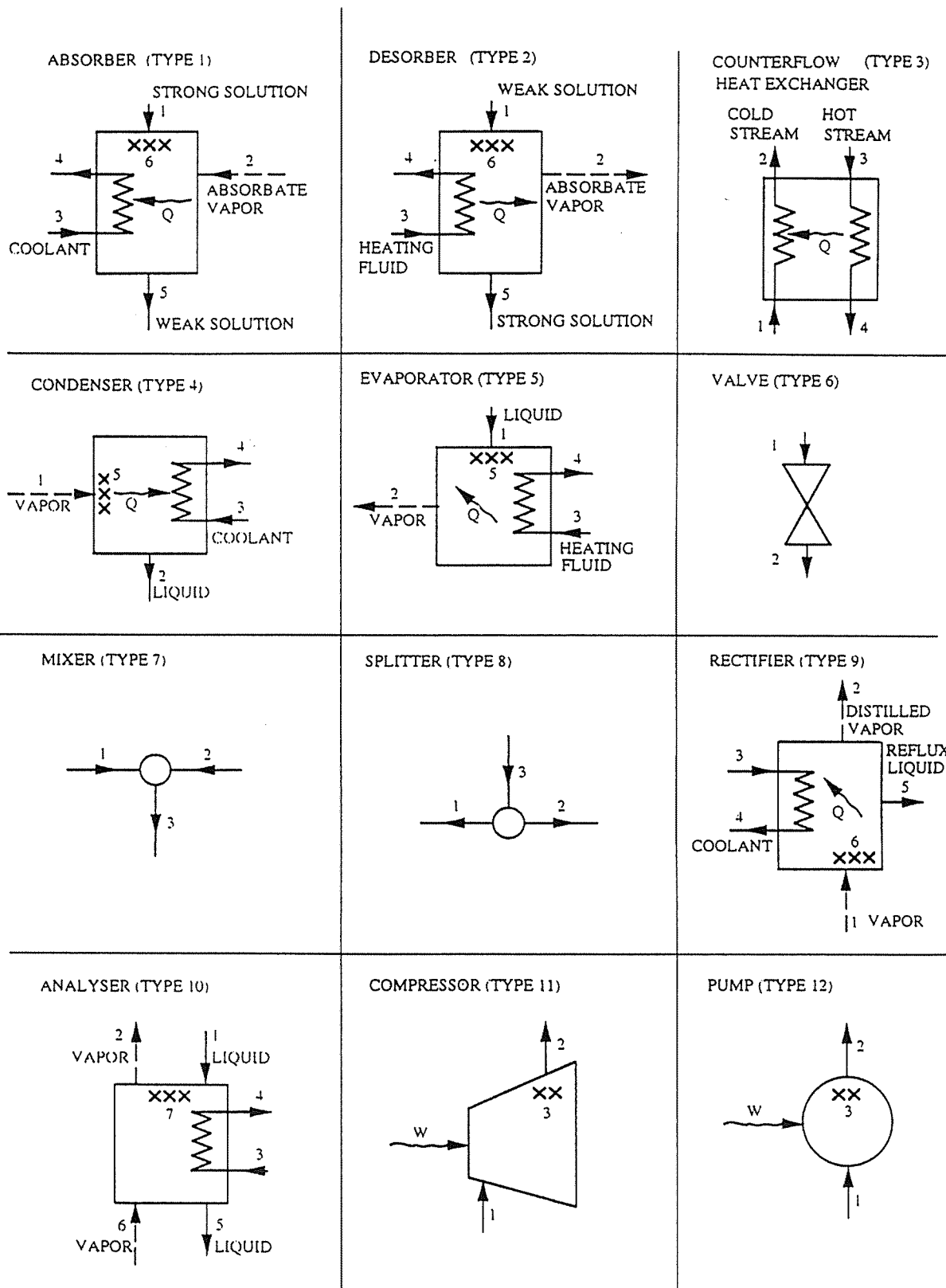


Fig. 2. Schematic description of individual components forming absorption systems.

and \overline{EEF} , \overline{CAT} , and \overline{LMTD} , are calculated values of these quantities in terms of the temperature at the unit's state points.

e. Vapor pressure-temperature-concentration (PTX) equilibrium between liquid and vapor:

$$f(P_i, T_i, C_i) = 0 . \quad (5)$$

f. Mass transfer, expressed in terms of temperature deviation from equilibrium (DEV):

$$T_i = T_{ie}(P_i, C_i) + DEV . \quad (6)$$

From the above equations for each unit, a set of nonlinear equations is formed for the entire system that must be solved simultaneously. This is done by expressing the equations in the form of functions whose residuals must be reduced by the solver to zero or, in practice, to a value below a given tolerance:

$$\begin{aligned} R_1(X_1, X_2, \dots, X_n) &= \varepsilon_1 . \\ R_2(X_1, X_2, \dots, X_n) &= \varepsilon_2 . \\ &\vdots \\ R_i(X_1, X_2, \dots, X_n) &= \varepsilon_i . \\ &\vdots \\ R_n(X_1, X_2, \dots, X_n) &= \varepsilon_n . \end{aligned} \quad (7)$$

$$|\varepsilon_i| \rightarrow 0 \text{ at the solution .}$$

As an example, consider the governing equations for the unit Analyzer (type 10)—a heat and mass exchanger common in ammonia-water systems. This unit was not part of earlier versions of the code but has been added to the current version. Figure 2 illustrates the Analyzer with its seven state points. A stream of liquid solution entering at state 1, possibly superheated or subcooled, reaches equilibrium at state 7 and leaves at state 5. It interacts with a stream of vapor entering at state 6 and leaving at state 2, in counterflow to the liquid. Heat may be added or removed in indirect contact through the stream (states 3→4).

Considering the Analyzer alone, one assumes that the fluid properties at all the inlet streams (1, 6, and 3) are known. The pressure in the Analyzer is assumed to be uniform and therefore fixed by the inlet streams for the outlet ones. The vapor leaving at state 2 is assumed to be in

thermal equilibrium with the incoming liquid at 1 (or 7), and its temperature is known. If the incoming liquid is neither subcooled nor superheated, states 1 and 7 are identical, and the flow and concentration at 2, the temperature, flow, and concentration at 5, and the temperature at 4—a total of six unknowns—remain to be found, requiring six physical equations as follows:

a. Conservation of total mass:

$$F_1 + F_6 - F_2 - F_5 = 0 . \quad (8)$$

b. Conservation of absorbent mass:

$$F_1 C_1 + F_6 C_6 - F_2 C_2 - F_5 C_5 = 0 . \quad (9)$$

c. Thermodynamic equilibrium (with possible temperature deviation) at liquid outlet 5:

$$T_{5E}(P_5, C_5) - T_5 + DEV = 0 . \quad (10)$$

d. Thermodynamic equilibrium at vapor outlet 2:

$$C_{2E}(P_2, T_2) - C_2 = 0 . \quad (11)$$

e. Heat balance:

$$F_1 h_1 + F_6 h_6 - F_2 h_2 - F_5 h_5 - F_3 (h_4 - h_3) = 0 . \quad (12)$$

f. Heat transfer, expressed by one of the four options in Eq. (4). If the user chooses to specify, say, the LMTD, Eq. (4d) becomes

$$LMTD - \frac{(T_4 - T_7) - (T_3 - T_5)}{\ln\left(\frac{T_4 - T_7}{T_3 - T_5}\right)} = 0 . \quad (13)$$

If the inlet stream 1 is either subcooled or superheated, three additional equations are generated for the temperature, flow, and concentration at 7. These are obtained from thermodynamic equilibrium at 7 and from heat and mass balances for the adiabatic absorption or

desorption process occurring, while the inlet stream 1 (subcooled or superheated, respectively) attempts to reach equilibrium [9].

Two of the twelve units—Compressor (type 11) and Pump (type 12)—are mechanical devices that require, in part, governing equations other than those in the set (1)–(6). Instead of heat transfer characteristics, the user specifies an isentropic efficiency for these units. Instead of a heat transfer equation, a compression equation is given, linking the change in enthalpy to the change in pressure. Instead of the heat duty, the output contains the work of compression.

By its nature, a system of simultaneous nonlinear equations may have more than one solution. One of the main problems in developing the code has been to ensure the physical solution regardless of the starting point. To do this, constraints were introduced into the program. The constraints are of inequality type and are generated by the unit subroutines when called, in much the same way as the equations. Each unit has its own constraints ensuring, for example, that the heat flow is from a hot to a cold stream and not vice versa. Thus, in the foregoing example, the constraints for the Analyzer, when heated externally, are

$$\left. \begin{array}{l} T_3 > T_5 \\ T_4 > T_7 \\ T_3 \geq T_4 \end{array} \right\} . \quad (14)$$

4. MATERIAL PROPERTIES

As mentioned earlier, the thermodynamic properties of working fluids have been incorporated into the code in the form of a property data base external to the unit subroutines. The purpose of doing so was twofold: first, to enhance modularity and flexibility by allowing different parts of a system to operate with different working fluids; and second, to allow for extension of the data base in the future and for adding properties of additional materials without affecting the rest of the code. Under this approach, each unit subroutine, when invoked, calls the data base several times and retrieves from it the properties required by its various equations. Also, the material may vary from one state point to another, as specified by the user.

The structure of the property data base has been described in detail in ref. [7]. For given pressure and liquid concentration, the property data base produces information on equilibrium temperature, equilibrium vapor concentration, and liquid and vapor enthalpies. For some of the materials, vapor entropy and liquid density have been added for calculating compression work in the Compressor and Pump units. The thermodynamic properties have been extracted from the literature, with references given in ref. [7].

The property data base currently contains the following materials:

<u>Material Code</u>	<u>Material</u>
1	LiBr-H ₂ O solution
2	H ₂ O-NH ₃ solution and vapor
3	H ₂ O liquid and vapor
4	LiBr-H ₂ O-NH ₃ solution
5	LiBr/ZnBr ₂ -CH ₃ OH solution
6	CH ₃ OH liquid and vapor
7	LiNO ₃ /KNO ₃ /NaNO ₃ -H ₂ O solution
8	NaOH-H ₂ O solution
9	LiCl-H ₂ O solution

5. CONSTRUCTION OF MATHEMATICAL MODEL

The process by which the physical behavior of the absorption system to be simulated is translated by the code into governing equations has been described in the preceding section. The equations are expressed in the form of functions whose residuals at the solution are to vanish. Some of the equations are highly nonlinear, and the set therefore can have more than one mathematical solution. Also, the code often generates redundant equations due to multiple mass balances from different units within a closed loop. To solve this problem, therefore, it is necessary to (1) identify and eliminate redundant equations, (2) apply constraints and define the feasible region for the physically valid solution, and (3) apply algorithms for solving the constrained set of equations.

The technique of solution was the bottleneck in earlier versions of the code [6, 7]. With complex cycles generating large sets of equations, the solver was unable to handle the task and achieve convergence. This was true particularly with systems employing working fluids with highly nonlinear properties, such as ammonia-water. In the current version, a great deal of attention was devoted to the mathematical part of the code, which has been enhanced considerably.

The first step toward the solution is a properly constructed mathematical model of the cycle. To this end, the unit subroutines in the code are employed in two different modes: first, to retrieve and construct the system of equations describing the entire cycle and the constraints on the variables; second, in the solver, to calculate the residual values of the functions for the physical variables within the feasible region.

After reading the input data, the main program begins building the mathematical model of the cycle. This process is accompanied by testing of the correctness of the input data. First, scaled mathematical variables $X = (X_1, X_2, \dots, X_n)$ are defined corresponding to the physical quantities to be calculated. Then, by calling the unit subroutines, the set of nonlinear equations

$$R(X) = 0 \quad (15)$$

is formed, where $R = (R_1, R_2, \dots, R_m)$. Also, physical constraints are imposed on the variables in the form of upper and lower bounds,

$$A_i > X_i > B_i, \quad i = 1, n, \quad (16)$$

and so-called diagonal constraints,

$$X_i > X_j, \quad (17)$$

for certain i and j . (An example of the latter constraint is the requirement set by the Second Law of Thermodynamics for the temperature at point i to be higher than that at point j if heat flows from point i to point j).

For a correctly defined cycle, the system in Eq. (15) should be neither over determined nor underdetermined. In the process of constructing the system in Eq. (15), two types of redundant equations may appear: linearly dependent equations (resulting from total and specific mass balances, which are interdependent due to the existence of closed loops in the cycle) and sometimes nonlinear duplicate equations. These redundant equations are identified and eliminated explicitly from the system in Eq. (15).

An absorption cycle may be treated as an oriented graph or network in which units—nodes and connections—are directed edges. Our linear equations describe the stream distribution in the nodes of the graph, and the number of independent equations is equal to the rank of the incidence matrix of the graph. This matrix is formed, and a Gauss elimination procedure is applied to select and eliminate the linearly dependent equations. This procedure is used separately for the truly linear equations of total mass balance and then in a somewhat more sophisticated form for the "quasi" linear equations of specific material mass balance.

Sometimes, for a definite structure of the cycle, the simulation program generates a number of duplicate nonlinear equations. A very simple method is employed for elimination of these equations. At the feasible initial point X_0 , the values of the functions $R_i(X)$ and the Jacobian $J(X_0)$ are calculated. If some functions have the same values and the elements of the derivatives are also the same, this indicates that these functions are duplicate; redundant ones are eliminated from the system in Eq. (15).

As a result of the above two procedures, we are able to obtain, for a correctly defined absorption cycle, the system in Eq. (15) with an equal number of equations and unknowns ($m = n$). If this condition is not satisfied, we obtain a diagnostic criterion of improper cycle definition in the input data. Elimination of redundant equations supplies the solver with a well-defined system.

The physical nature of the problem causes the Jacobian of the system in Eq. (15) to be sparse, involving usually no more than 10–25% nonzero elements. During the solution process, the finite difference approximation of the Jacobian is calculated several times, which takes n evaluations of all the functions $R_i(X)$. Using the sparsity pattern of the Jacobian makes it possible to significantly reduce the number of function evaluations for building the approximation with respect to filling of nonzero elements. Therefore, on the last step of constructing the mathematical model, the code builds the sparsity pattern of the Jacobian $J(X)$.

6. ALGORITHM OF SOLUTION

The problem of calculating the performance parameters of an absorption cycle has been reduced to the solution of a well-defined system of nonlinear algebraic equations [Eq. (15)] with the constraints in Eq. (16) and Eq. (17). Four characteristic features of the problem are as follows:

- the number, type, and order of the equations vary from one case to another, depending on the cycle and working fluids;
- some of the functions in the system are not defined explicitly;
- the residuals can be calculated only within the feasible region [Eqs.(16)–(17)] by the unit subroutines; and
- for calculation of some functions, it is necessary to call the property data base, a task that is often time consuming.

An extensive search among available software has revealed no algorithms for solution of systems of nonlinear equations with constraints of the present type; ref. [10] emphasizes the need for their development. Standard methods of constrained optimization do not accommodate the specific features of the present problem, and algorithms of nonlinear least squares with linear constraints [11] presume an analytical calculation of the Jacobian; this is unacceptable for the present problem. We therefore preferred to use an algorithm for solving simultaneously a system of nonlinear equations with numerical approximation of the Jacobian and to adapt it to the constrained situation by projection on the feasible region.

As a basic method for solving the system of nonlinear equations, a hybrid algorithm for unconstrained systems that was developed by Powell [12] has been employed. This method combines quasi-Newton and gradient approaches. Such a combination makes it possible to avoid complications due to a singular Jacobian and to reduce the strict requirements on the initial guess. At the same time, the hybrid algorithm retains the efficiency of a quasi-Newton method.

The hybrid algorithm has been described in detail in ref. [12]; it is an iterative algorithm in which each step is constrained by a repeatedly adjusted value Δ_k —which defines a so-called "trust region." For the current iterate, the displacement δ_k of X^k is selected according to the following logic. Two searching directions are considered: first, the Newton step, which has the form

$$\delta_n = -J^{-1}(X^k) * R(X^k), \quad (18)$$

where $J(X^k)$ is an approximation of the Jacobian at the X^k ; and second, the steepest descent step toward the minimum of the function

$$f(X) = \sum [R_i(X)]^2 \quad (19)$$

along the antigradient direction that can be expressed as

$$g = -\beta * J^T(X^k) * R(X^k) \quad (20)$$

for definite $\beta > 0$. If $\|\delta_n\| < \Delta_k$, the step δ_k is just the classical Newton correction: $\delta_k = \delta_n$. If the inequality does not hold, the step in Eq. (20) is tested. If $\|g\| > \Delta_k$, then the step of the length Δ_k along the antigradient is executed. However, if $\|g\| < \Delta_k$, the displacement has also the length Δ_k and is a linear combination of the Newton and gradient steps. The actual displacement to the new point $X^{k+1} = X^k + \delta_k$ is realized only if

$$f(X^{k+1}) < f(X^k) . \quad (21)$$

The hybrid method uses a numerical approximation of the Jacobian $J(X)$ that is updated at each iteration and recalculated by finite differences when necessary. Special conditions for adjusting Δ_k and updating the approximation of the Jacobian ensure convergence and efficiency of the hybrid algorithm [12].

For the constrained problem, the current point X^k should be inside the feasible region. There are several different approaches for keeping the current point feasible. We ensure the feasibility by projection on the polyhedron defined by the constraints in Eqs.(16)–(17). Vector δ_k is calculated as in the original hybrid method. The point $X_k + \delta_k$ is tested for feasibility and, if certain constraints are violated, the orthogonal projection X_{Pr} is calculated. The next stage of iteration is to try to estimate $f(X_{Pr})$; the functions $R_i(X_{Pr})$, $i = 1, n$ are therefore calculated at this point. If the expected inequality $f(X_{Pr}) < f(X^k)$ holds, then the iteration defines $X^{k+1} = X_{Pr}$. However, if this condition fails, we let $X^{k+1} = X^k$ and reduce the step-length restrictor Δ^k . Due to the logic of the hybrid method, if Δ_k is small enough, the searching direction coincides with the antigradient direction for function $f(X)$. In this case, one can take advantage of the gradient projection algorithm [13], which converges to the minimum of $f(X)$. This convergence ensures a decrease of the function $f(X)$ and provides a criterion of existence of nonzero minimum $f(X)$ on the boundaries. In the latter case, the algorithm stops and recommends that the user repeat the calculation with another initial guess.

The rules for adjusting the step-length restrictor Δ_k and reevaluating the Jacobian by finite difference approximation are chosen so as to reduce the amount of work spent on searching the exact minimum of $f(X)$ on the boundaries.

The procedure of testing the current point for feasibility and projecting it on the feasible region is implemented in a separate subroutine. The existence of the diagonal constraints (17) makes this task nontrivial but still simpler than in the case of common linear constraints. For orthogonal projection, a method of quadratic programming is employed [13], which comprises successive solutions of the system of linear equations. For our case, these systems are very sparse; an algorithm has been selected [14] that can take advantage of this sparsity.

The new algorithm was applied to the solution of sets of the system in Eqs.(15)–(17) for different types of absorption cycles. Results of calculations show fast and reliable convergence to the solution and only a weak dependence of the convergence properties of the algorithm on the initial guess for such tasks. After checking the algorithm on some test problems, we would recommend it for other applications.

7. SIMULATION RESULTS

Before the program was used extensively for analysis of various advanced cycles, several initial runs were made for validation against experimental data taken on working absorption systems. Unfortunately, good documented data are quite scarce. The literature describes a number of absorption systems developed during the past two decades, but only limited information is given on their heat transfer characteristics, with test data confined to a narrow range around the design point. Experimental data for our validation of the program were selected from measurements on an LiBr-H₂O heat transformer for upgrading waste heat and were developed and tested extensively at Oak Ridge National Laboratory (ORNL) [15]. Seventy-three experimental runs were documented in which the machine had operated under steady-state, stable conditions for 1 to 8 h. The results of the validation have been described in detail in ref. [6]. Very good agreement was obtained between the simulation and experimental results.

Earlier versions of the code have been used to simulate more than 30 various cycles of interest with the working fluids LiBr-H₂O, H₂O-NH₃, LiBr-H₂O-NH₃, and LiBr/ZnBr₂-CH₃OH. These cycles included single-effect, double-effect, and dual-loop chillers, heat pumps, and heat transformers in various configurations. Some results for typical cases showing design point performance have been described in ref. [7]. Most systems with a working fluid involving a nonvolatile absorbent usually converged without difficulty; some problems were encountered concerning fluids with a volatile absorbent such as H₂O-NH₃ due to the highly nonlinear behavior of these materials at large concentrations of the volatile component in the vapor phase. The mathematical improvements in the present version of the code were designed primarily to deal with these problems.

An earlier version of the code has been employed to conduct a detailed parametric study to investigate the performance of various cycles using LiBr-H₂O [16], a fluid pair of much practical interest. Complete performance maps under varying operating conditions have been generated for systems in single-stage and several double-stage configurations, in series and in parallel connection. The lack of flexibility in system-specific simulation models may be the reason why only a few comparative studies of advanced cycles have been carried out to date [17, 18]. In the published literature describing these studies, a cycle's performance is often characterized by no more than a single point. Here, the performance has been compared over the entire temperature domain applicable to the cycle. Figure 3 shows a set of curves typical of those calculated in ref. [16], describing COP as a function of operating temperatures with a comparison to Carnot. It is evident that for each cooling water temperature there exists a minimum temperature of the supply heat below which the COP vanishes, and that this minimum is higher for a double-effect system than for a single-effect one. With increasing heat supply temperature, the COP increases rapidly at

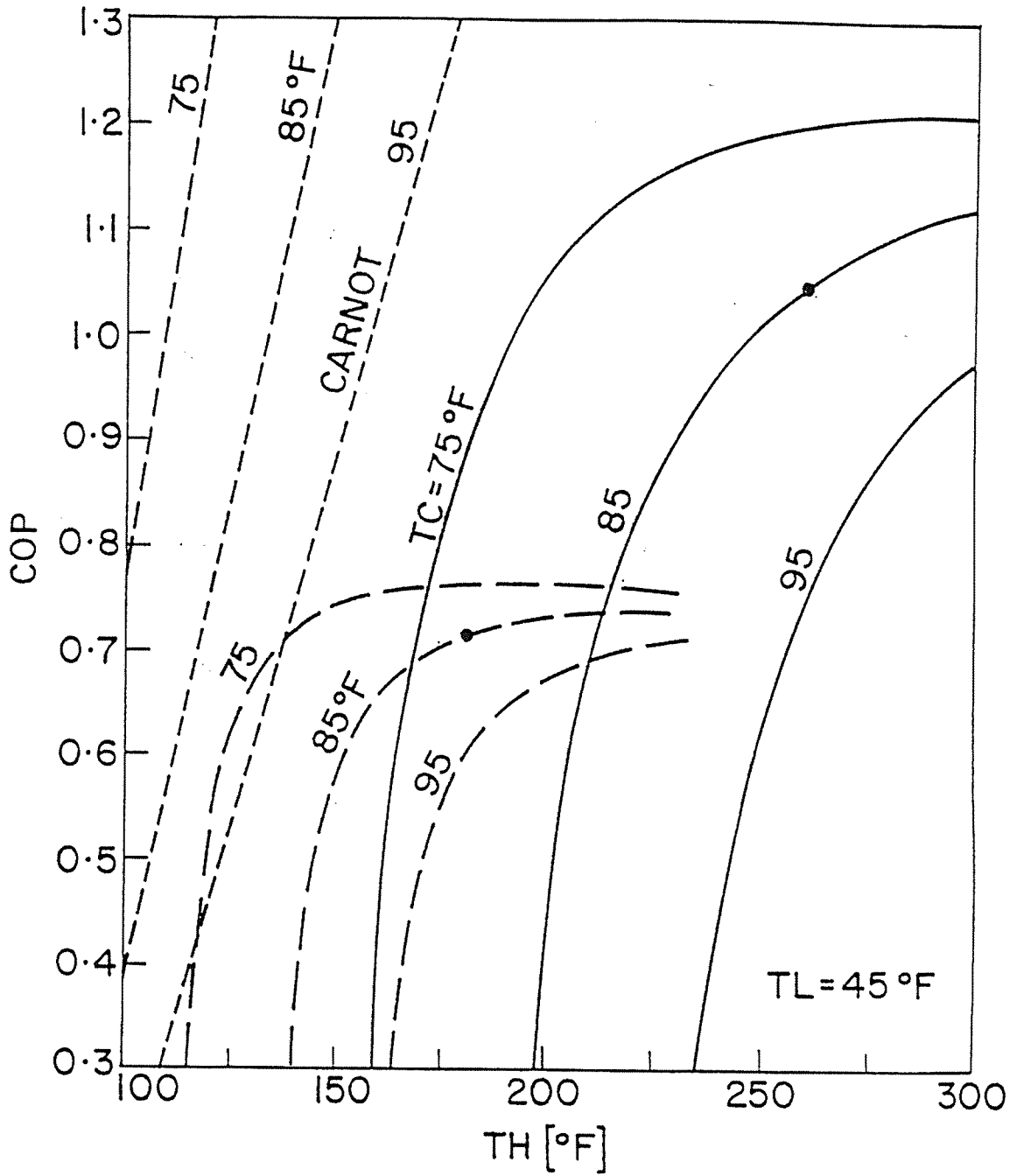
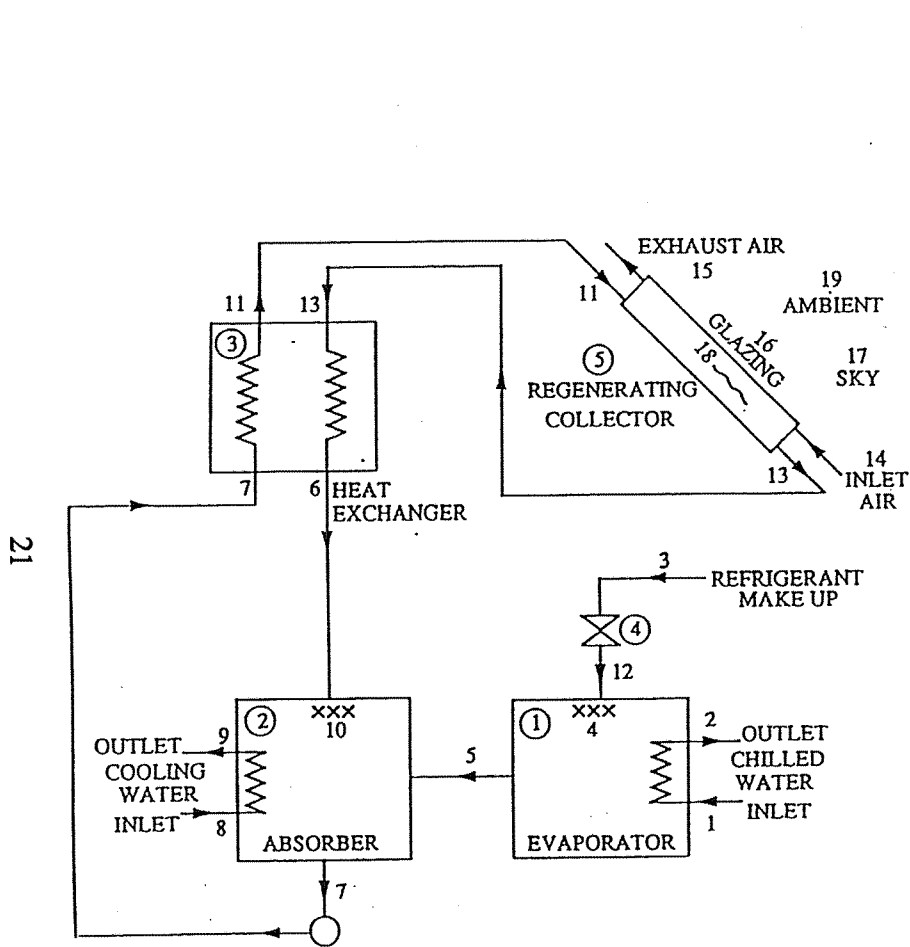


Fig. 3. Coefficient of performance (COP) for double-effect, series flow system (solid lines) and single-effect system (broken lines) as functions of operating temperatures. Carnot COP for the same operating conditions is given for comparison.

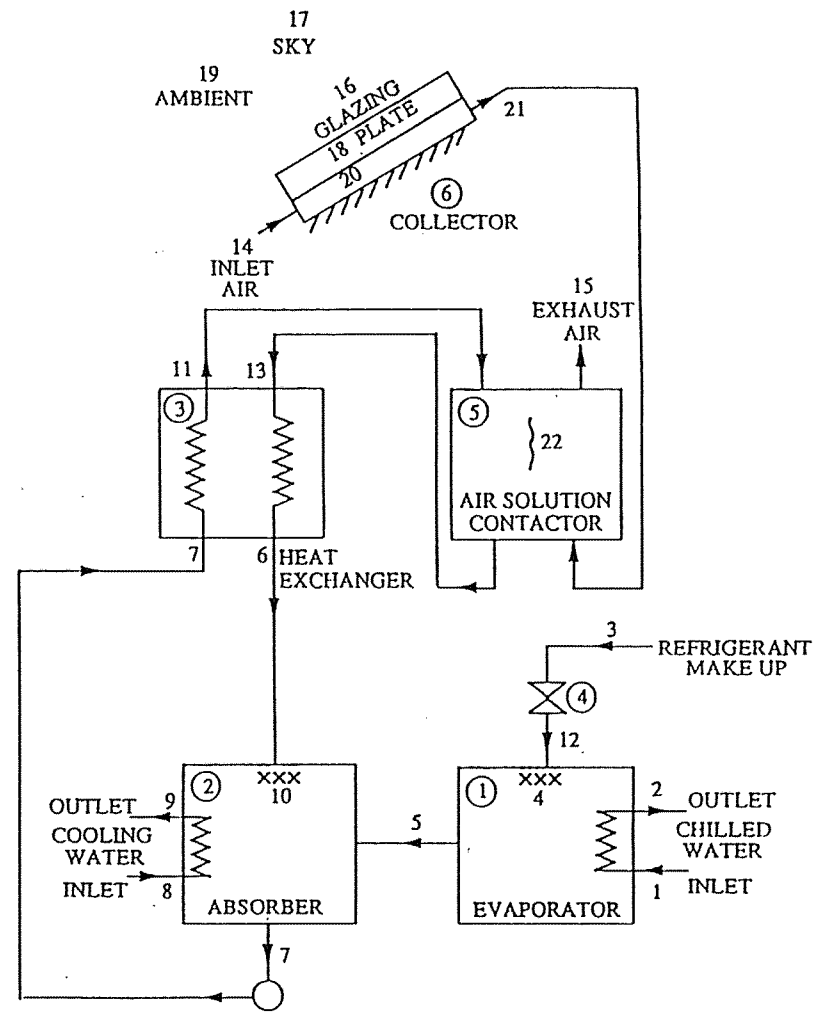
first, then levels off and even declines slightly; a switch from single to double-effect is then in order. The reason for this behavior has been discussed in ref. [17]. The effect of other operating parameters, such as solution flow rate and heat transfer area in the different components, has been investigated. The thermodynamic potential of LiBr-H₂O has been studied and compared with that of other absorption fluid pairs.

The present version of the code made it possible to simulate cycles with a degree of complexity never attempted before. The LiBr-H₂O study [16] of single- and double-effect systems has been extended to triple-effect cycles. Figure 4 describes two triple-effect chillers, in parallel and in series connection. These were formed as an extension of the corresponding double-effect systems in ref. [16] by maintaining the same heat transfer characteristics and adding one desorber, one condenser, and one heat exchanger of the same size as in ref. [16]. Cooling is produced in Evaporator 1, fed by water condensate from three condensers, while high-temperature heat from an external source is supplied to Desorber 13 only. Desorbers 3 and 4 are powered by reject heat from Condensers 6 and 14, respectively, as shown. Calculation results for a typical design point (500°F heat supply, 85°F cooling water supply, and 45°F chilled water output) are given in Tables A-1 and A-2 in Appendix A for the two cycles. The parallel flow system yields a higher COP than the series system, under the same operating conditions, as has been the case for the double-effect cycles in [16]. Additional configurations of triple-effect cycles with LiBr-H₂O, employing more sophisticated methods of internal heat recovery, have been simulated.

Another study [19] has employed the code to perform a comparative simulation of two open-cycle absorption systems for solar cooling. Such systems have been under development in parallel for the past few years [20, 21]. The systems are described schematically in Fig. 5. The working fluid in both is LiCl-H₂O, where the water desorbs into the atmosphere and is replaceable. Both systems comprise a closed absorber and evaporator as in conventional, single-stage absorption chillers. The open part of the cycle is in the regenerator, used to reconcentrate the absorbent solution by means of solar energy. One of the systems under study [20] has employed direct regeneration (DR) in a regenerating collector, exposing the solution simultaneously to the sun and to a stream of air. The other system [21] has employed indirect regeneration (IR) by bringing the solution into contact with air heated elsewhere in a flat plate collector. To perform the simulation, unit subroutines for solar components—air heating collector, air solution contactor, and regenerating collector—were added to the code, and its property data base was expanded to include properties of moist air. The code was applied first to study the behavior of these newly added individual components, and then to evaluate the performance of the complete open-cycle absorption systems. The simulation yielded two measures of performance—COP and capacity—as functions of the operating parameters. Performance maps similar to those in Fig. 3 were drawn over the entire applicable domain. The behavior of both systems was observed to be qualitatively



(a)



(b)

Fig. 5. Schematic description of solar powered open absorption systems.
 (a) direct regeneration, (b) indirect regeneration.

similar; however, COP values in the IR system were considerably lower than those in the DR one. The primary reason for this is that the DR system employs direct heating of the solution during regeneration whereby solar heat is provided where needed, while the IR system heats air that then has to transfer the heat to the solution, leading to greater losses.

Another working fluid pair of great practical interest is ammonia-water. It is well known that due to the volatile nature of the absorbent (water) and the relatively high vapor pressure of the refrigerant (ammonia), systems employing this working pair must be designed differently from those with LiBr-H₂O. In particular, rectification must generally be provided downstream of the desorber. As mentioned earlier, the volatile absorbent results in highly nonlinear behavior of the properties, which makes the solution of the equations generated by the simulation code very difficult. The enhanced algorithm in the current version of the code has made it possible to simulate a variety of ammonia-water heat pumps and heat transformers. Figure 6 shows a single-effect ammonia-water chiller involving a rectifier (7) and a recuperative heat exchanger (10) from liquid to vapor refrigerant. Evaporator 1 is actually a desorber, allowing for some liquid refrigerant to leave unevaporated. Calculation results for a typical design point are given in Table A-3 in Appendix A.

One of the main absorption programs in the United States is currently developing a residential heat pump based on the GAX cycle [22]. When using a working fluid with a wide solution field such as ammonia-water in a single-stage system with a high regeneration temperature, some temperature overlap exists between the absorber and desorber, making it possible to recover heat from the former to the latter and to obtain some "free" regeneration. The possibility of using GAX in combination with a solution-cooled absorber and a solution-heated generator is described in detail in ref. [22] and has been contemplated for some time. Some simplified calculations were performed for COP estimation under Phase 1 of the U.S. Department of Energy (DOE)/ORNL advanced cycles development program [22]. However, a detailed calculation has been a formidable task due to the complexity of the cycle combined with the highly nonlinear nature of the NH₃-H₂O working fluid. The current version of the code has made it possible recently to perform such detailed simulation. Figure 7 describes the GAX heat pump in terms of the units recognizable by the code. The absorber and desorber are each split into three parts. Absorber 12 is externally cooled, Absorber 11 is solution cooled, and Absorber 5 is GAX cooled; similarly, Desorber 3 is externally heated, Desorber 2 is solution heated, and Desorber 13 is GAX heated, as shown. Calculation results for a typical cooling condition are given in Table A-4 in Appendix A.

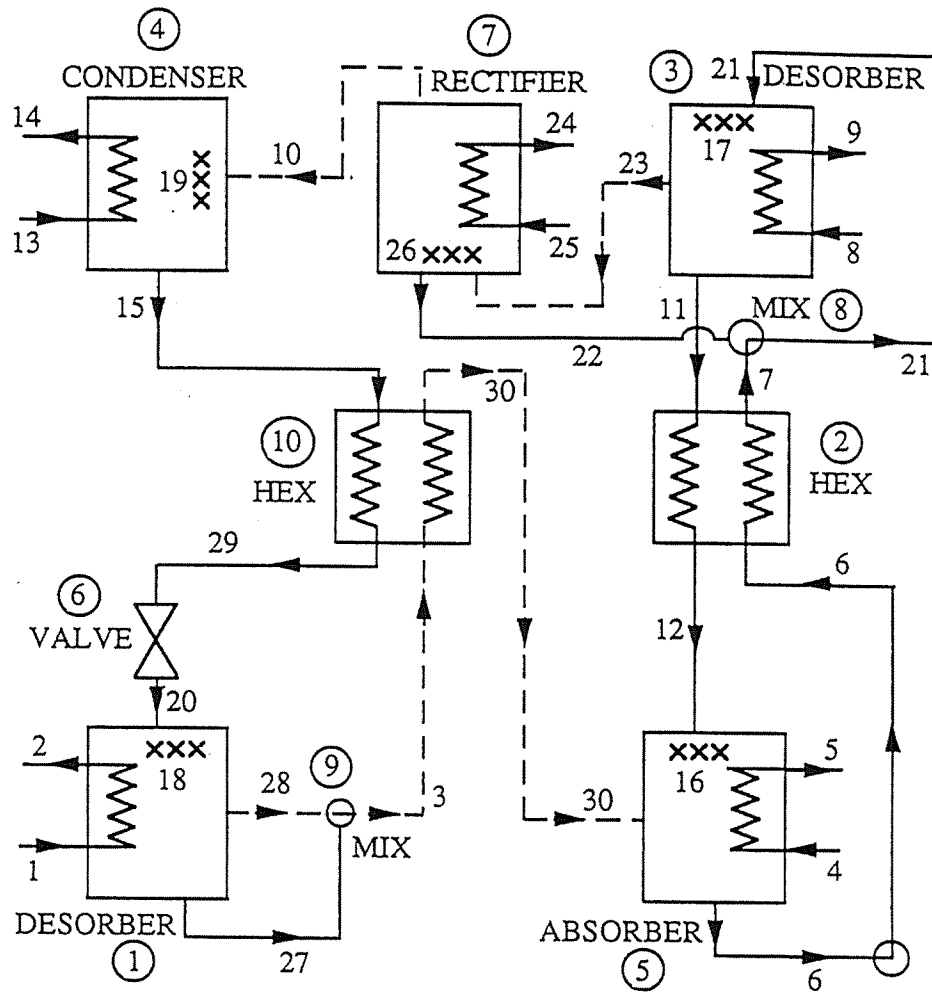


Fig. 6. Schematic description of single effect ammonia-water system.

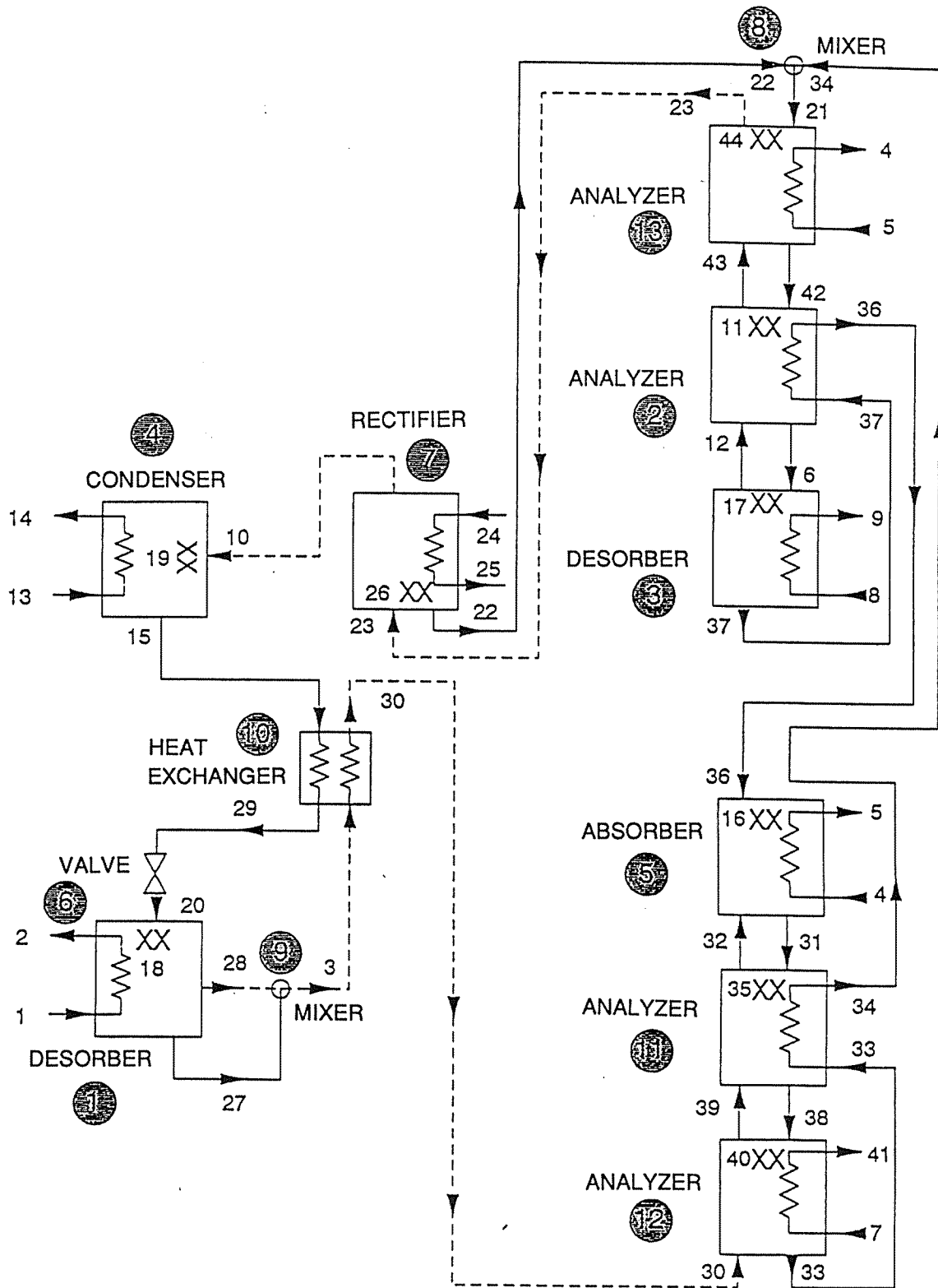


Fig. 7. Schematic description of ammonia-water generator-absorber heat exchange (GAX) cycle.

8. CONCLUSION

The improvements made to the present version of the code have significantly enhanced its capabilities compared with earlier versions. The code was used successfully in calculating various new absorption cycles, including rather complex ones: triple-effect chillers in several configurations with lithium bromide-water as the working pair, and GAX heat pumps with ammonia-water as a working fluid. The mathematical model for these cycles produces about 60 equations and around 40 constraints of the type in Eq. (17). The solver successfully copes with such rather large problems. It takes about 20 iterations of the algorithm and about 30 function evaluations to get the solution; these values do not depend very much on the initial guess. Results of calculations show that the above changes to the original computer code have made it more reliable and effective than ever before.

9. REFERENCES

1. G. C. Vliet, M. B. Lawson, and R. A. Lithgow, "Water-Lithium Bromide Double Effect Absorption Cooling Cycle Analysis," *ASHRAE Transactions* **88**(1), 811–823 (1982).
2. G. Grossman, et al., "Solar Powered Environment Control Criteria and Realization," pp. 720–724 in *Proceedings—The 1979 International Solar Energy Society Conference*, Atlanta, May 1979, K. W. Boer and B. H. Glenn, eds., Pergamon, Elmsford, N.Y., 1979.
3. G. Grossman and K. W. Childs, "Computer Simulation of a Lithium Bromide-Water Absorption Heat Pump for Temperature Boosting," *ASHRAE Trans.* **89**(1b), 240–248 (1983).
4. M. O. McLinden and S. A. Klein, "Steady State Modeling of Absorption Heat Pumps with a Comparison to Experiments," *ASHRAE Trans.* **91**(2b), 1793–1807 (1985).
5. H. Perez-Blanco and M. R. Patterson, *Conceptual Design and Optimization of a Versatile Absorption Heat Transformer*, ORNL/TM-9841, Oak Ridge National Laboratory, Oak Ridge, Tenn., 1986.
6. G. Grossman and E. Michelson, "A Modular Computer Simulation of Absorption Systems," *ASHRAE Trans.* **91**(2b), 1808–1827 (1985). Also ORNL/Sub/83-43337/2, Oak Ridge National Laboratory, Oak Ridge, Tenn., 1986.
7. G. Grossman, K. Gommed, and D. Gadoth, "A Computer Model for Simulation of Absorption Systems in Flexible and Modular Form," *ASHRAE Trans.* **93**(2), 2389–2428 (1987). Also ORNL/Sub/90-89673, Oak Ridge National Laboratory, Oak Ridge, Tenn., 1990.
8. G. Grossman, "Computer Simulation and Analysis of Absorption Systems," pp. 203–209 in *Proceedings of the Meeting on Thermophysical Properties of Pure Substances and Mixtures for Refrigeration*, Commission B1 of the International Institute of Refrigeration, Herzelia, Israel, March 5–7, 1990.
9. G. Grossman, "Adiabatic Absorption and Desorption for Improvement of Temperature-Boosting Absorption Heat Pumps," *ASHRAE Trans.* **88**(2), 359–367 (1982).
10. K. L. Hiebert, "An Evaluation of Mathematical Software that Solves Systems of Nonlinear Equations," *Association for Computing Machinery Transactions on Mathematical Software (ACM TOMS)* **8**, 5–20 (1982).
11. S. J. Wright and J. N. Holt, "Algorithms for Nonlinear Least Squares with Linear Inequality Constraints," *SIAM J. of Sci. Stat. Comput.* **6**(4), 1033–1048 (1985).
12. M. J. D. Powell, "A Hybrid Method for Nonlinear Equations," pp. 87–114 in *Numerical Methods for Nonlinear Algebraic Equations*, ed. P. Rabinowitz, Gordon & Breach, London, 1970.

13. B. T. Polyak, *Introduction to Optimization* (in Russian), Nauka, Moscow, 1983, pp. 296–300.
14. J. K. Reid, *Two Fortran Subroutines for Direct Solution of Linear Equations Whose Matrix is Sparse, Symmetric and Positive-Definite*, Atomic Energy Research Establishment (AERE) Report R-7119, 1971.
15. W. R. Huntley, "Performance Test Results of an Absorption Heat Pump Using Low Temperature (60°C) Industrial Waste Heat," pp. 1921–1926 in *Proceedings of the 18th Intersociety Energy Conversion Engineering Conference (IECEC), Orlando, Fla., August 1983*, Vol. 4, 1983. Also ORNL/TM-9072, Oak Ridge National Laboratory, Oak Ridge, Tenn., 1984.
16. K. Gomme and G. Grossman, "Performance Analysis of Staged Absorption Heat Pumps: Water-Lithium Bromide Systems," *ASHRAE Trans.* **96**(1), 1590–1598 (1990).
17. W. J. Biermann, *Advanced Absorption Heat Pump Cycles*, ORNL/Sub/81-17499/1, Oak Ridge National Laboratory, Oak Ridge, Tenn., (in press).
18. B. A. Phillips, "Analysis of Advanced Residential Absorption Heat Pump Cycles," pp. 265–231 in *Proceedings of the DOE/ORNL Heat Pump Conference, Washington D.C., December 1984*, Oak Ridge National Laboratory, Oak Ridge, Tenn., 1985.
19. I. Haim, G. Grossman, and A. Shavit, "Simulation and Analysis of Open Cycle Absorption Systems for Solar Cooling," pp. 1607–1612 in *Proceedings of the Biennial Congress 1991 International Solar Energy Society, Denver, August 19–23, 1991*, Vol. 2, part 1, Pergamon, Elmsford, N.Y., 1991.
20. B. D. Wood, *Open Cycle Absorption Solar Cooling*, Final Report, No. ERC-R-86020D, College of Engineering and Applied Sciences, Arizona State University, Tempe, Ariz., 1986.
21. T. G. Lenz, et al., *Open Cycle Lithium Chloride Cooling System*, Final Reports on DOE Contract for 1982/83 and 1983/84, Solar Energy Applications Laboratory, Colorado State University, Ft. Collins, Colo., 1983 and 1985.
22. B. A. Phillips, "Development of a Gas-Fired Heat Pump with an Improved Absorption Cycle," pp. 97–102 in *Proceedings of the 1988 ASME Winter Annual Meeting, Chicago, November 27–December 2, 1988 (Analysis and Applications of Heat Pumps, Vol. AES-8/SED-6)*, American Society of Mechanical Engineers, 1988.

ACKNOWLEDGMENTS

The authors are grateful to F. A. Creswick and R. C. DeVault for many useful suggestions. The project was sponsored by ORNL for DOE under Contract No. 19X-SH641V.

**Enhanced Absorption Cycle Computer Model
Appendix A
Results of Calculations**

APPENDIX A: RESULTS OF CALCULATIONS

Outputs are in British Units:

Temperatures (T) in °F
 Mass Flow Rates (F) in lb/min
 Concentrations (C) in wt %
 Enthalpies (H) in Btu/lb
 Pressures (P) in psia
 Heat Quantities (Q) in Btu/min

Table A-1. LiBr-H₂O 3-Effect Chiller Series Flow 1

State Point	Temper.	Enthalpy	Flow Rate	Concentr.	Pressure	Vapor Fr.
1	1.3940D+02	8.5393D+01	5.4746D+01	6.7863D+01	1.1628D-01	0.0000D+00
2	3.8833D+01	1.0781D+03	5.2543D+00	0.0000D+00	1.1628D-01	1.0000D+00
3	8.5000D+01	5.2890D+01	4.8300D+02	0.0000D+00	0.0000D+00	0.0000D+00
4	9.9042D+01	6.6859D+01	4.8300D+02	0.0000D+00	0.0000D+00	0.0000D+00
5	1.1613D+02	5.9872D+01	6.0000D+01	6.1920D+01	1.1628D-01	0.0000D+00
6	1.3813D+02	8.4949D+01	5.4721D+01	6.7894D+01	1.1628D-01	0.0000D+00
7	2.2308D+02	1.1987D+02	5.4746D+01	6.7863D+01	7.0499D-01	0.0000D+00
8	1.8634D+02	9.1330D+01	6.0000D+01	6.1920D+01	7.0499D-01	0.0000D+00
9	1.8357D+02	1.1422D+03	1.4666D+00	0.0000D+00	7.0499D-01	1.0000D+00
10	1.8901D+02	1.5700D+02	4.0000D+02	0.0000D+00	0.0000D+00	0.0000D+00
11	1.8490D+02	1.5285D+02	4.0000D+02	0.0000D+00	0.0000D+00	0.0000D+00
12	1.8357D+02	9.3340D+01	5.8533D+01	6.3472D+01	7.0499D-01	0.0000D+00
13	3.0109D+02	1.4483D+02	5.8533D+01	6.3472D+01	9.4091D+00	0.0000D+00
14	3.1328D+02	1.1974D+03	1.5965D+00	0.0000D+00	9.4091D+00	1.0000D+00
15	3.1903D+02	2.8923D+02	4.0000D+02	0.0000D+00	0.0000D+00	0.0000D+00
16	3.1384D+02	2.8390D+02	4.0000D+02	0.0000D+00	0.0000D+00	0.0000D+00
17	3.5667D+02	1.7492D+02	5.4746D+01	6.7863D+01	9.4091D+00	0.0000D+00
18	3.0318D+02	1.4568D+02	5.8581D+01	6.3421D+01	9.4091D+00	0.0000D+00
19	1.9036D+02	1.5836D+02	1.5965D+00	0.0000D+00	9.4091D+00	0.0000D+00
20	1.9036D+02	1.1421D+03	1.5965D+00	0.0000D+00	9.4091D+00	1.0000D+00
21	3.8833D+01	1.5836D+02	1.5965D+00	0.0000D+00	1.1628D-01	1.4119D-01
22	9.0338D+01	5.8197D+01	1.4666D+00	0.0000D+00	7.0499D-01	0.0000D+00
23	8.5000D+01	5.2890D+01	3.9100D+02	0.0000D+00	0.0000D+00	0.0000D+00
24	8.9090D+01	5.6956D+01	3.9100D+02	0.0000D+00	0.0000D+00	0.0000D+00
25	9.0338D+01	1.1003D+03	1.4666D+00	0.0000D+00	7.0499D-01	1.0000D+00
26	3.8833D+01	5.8197D+01	1.4666D+00	0.0000D+00	1.1628D-01	4.7663D-02
27	3.8833D+01	1.8572D+02	5.2543D+00	0.0000D+00	1.1628D-01	1.6674D-01
28	6.0796D+01	2.8876D+01	3.0000D+02	0.0000D+00	0.0000D+00	0.0000D+00
29	4.5000D+01	1.3247D+01	3.0000D+02	0.0000D+00	0.0000D+00	0.0000D+00
30	3.8833D+01	1.8572D+02	5.2543D+00	0.0000D+00	1.1628D-01	1.6674D-01
31	1.7790D+02	8.7954D+01	5.9808D+01	6.2119D+01	7.0499D-01	0.0000D+00
32	3.1328D+02	1.5273D+02	5.6937D+01	6.5252D+01	9.4091D+00	0.0000D+00
33	4.4003D+02	2.0690D+02	5.6937D+01	6.5252D+01	9.0628D+01	0.0000D+00
34	4.6732D+02	2.1820D+02	5.7553D+01	6.4553D+01	9.0628D+01	0.0000D+00
35	5.0000D+02	4.7713D+02	4.1600D+02	0.0000D+00	0.0000D+00	0.0000D+00
36	4.9165D+02	4.6836D+02	4.1600D+02	0.0000D+00	0.0000D+00	0.0000D+00
37	4.9337D+02	2.3126D+02	5.4746D+01	6.7863D+01	9.0628D+01	0.0000D+00
38	4.9337D+02	1.2631D+03	2.1912D+00	0.0000D+00	9.0628D+01	1.0000D+00

39	3.2078D+02	1.1854D+03	2.1912D+00	0.0000D+00	9.0628D+01	1.0000D+00
40	3.2078D+02	2.9102D+02	2.1912D+00	0.0000D+00	9.0628D+01	0.0000D+00
41	3.8833D+01	2.9102D+02	2.1912D+00	0.0000D+00	1.1628D-01	2.6507D-01
42	3.8833D+01	2.3510D+02	3.7877D+00	0.0000D+00	1.1628D-01	2.1285D-01

Equivalent Unit Heat Transfer Characteristics for Each Unit

No.	Type	UA	EFF	CAT	LMTD
1	Evaporator	3.7700D+02	7.1920D-01	6.1675D+00	1.2437D+01
2	Absorber	1.9300D+02	4.1400D-01	3.1134D+01	3.4959D+01
3	Desorber	2.6800D+02	5.1029D-01	5.4438D+00	6.1898D+00
4	Desorber	2.6800D+02	6.3748D-01	5.7444D+00	7.9478D+00
5	Condenser	5.6500D+02	7.6627D-01	1.2476D+00	2.8139D+00
6	Condenser	5.6500D+02	7.5379D-01	1.3441D+00	2.9361D+00
7	Heat Exger	6.4000D+01	7.8242D-01	2.3269D+01	2.9492D+01
8	Heat Exger	6.4000D+01	7.7176D-01	3.9510D+01	4.7092D+01
9	Mixer	0.0000D+00	0.0000D+00	0.0000D+00	0.0000D+00
10	Valve	0.0000D+00	0.0000D+00	0.0000D+00	0.0000D+00
11	Valve	0.0000D+00	0.0000D+00	0.0000D+00	0.0000D+00
12	Heat Exger	6.4000D+01	7.5907D-01	4.3389D+01	4.8195D+01
13	Desorber	2.6800D+02	7.9722D-01	6.6274D+00	1.3613D+01
14	Condenser	5.6500D+02	7.4775D-01	1.7517D+00	3.7699D+00
15	Valve	0.0000D+00	0.0000D+00	0.0000D+00	0.0000D+00
16	Mixer	0.0000D+00	0.0000D+00	0.0000D+00	0.0000D+00

No.	Type	Heat Transfer	Eq. Dev.	IPInch
1	Evaporator	4.6887D+03	0.000D+00	-1
2	Absorber	6.7471D+03	0.000D+00	-1
3	Desorber	1.6589D+03	0.000D+00	1
4	Desorber	2.1300D+03	0.000D+00	1
5	Condenser	1.5899D+03	0.000D+00	1
6	Condenser	1.6589D+03	0.000D+00	1
7	Heat Exger	1.8875D+03	0.000D+00	-1
8	Heat Exger	3.0139D+03	0.000D+00	-1
9	Mixer	0.0000D+00	0.000D+00	0
10	Valve	0.0000D+00	0.000D+00	0
11	Valve	0.0000D+00	0.000D+00	0
12	Heat Exger	3.0845D+03	0.000D+00	-1
13	Desorber	3.6483D+03	0.000D+00	1
14	Condenser	2.1300D+03	0.000D+00	1
15	Valve	0.0000D+00	0.000D+00	0
16	Mixer	0.0000D+00	0.000D+00	0

COP = 1.2852

Table A-2. LiBr-H₂O 3-Effect Chiller, Parallel Flow

State Point	Temper.	Enthalpy	Flow Rate	Concentr.	Pressure	Vapor Fr.
1	2803D+02	7.6611D+01	5.5139D+01	6.6347D+01	1.1874D-01	0.0000D+00
2	3.9366D+01	1.0783D+03	4.8613D+00	0.0000D+00	1.1874D-01	1.0000D+00
3	8.5000D+01	5.2890D+01	4.8300D+02	0.0000D+00	0.0000D+00	0.0000D+00
4	9.7672D+01	6.5495D+01	4.8300D+02	0.0000D+00	0.0000D+00	0.0000D+00
5	1.1330D+02	5.6301D+01	6.0000D+01	6.0972D+01	1.1874D-01	0.0000D+00
6	1.3270D+02	7.8276D+01	5.5230D+01	6.6237D+01	1.1874D-01	0.0000D+00
7	1.7852D+02	9.7817D+01	5.5139D+01	6.6347D+01	6.7436D-01	0.0000D+00
8	1.5618D+02	7.5788D+01	2.0000D+01	6.0972D+01	6.7436D-01	0.0000D+00

9	1.8599D+02	1.1433D+03	1.0753D+00	0.0000D+00	6.7436D-01	1.0000D+00
10	1.8769D+02	1.5567D+02	4.0000D+02	0.0000D+00	0.0000D+00	0.0000D+00
11	1.8387D+02	1.5182D+02	4.0000D+02	0.0000D+00	0.0000D+00	0.0000D+00
12	1.8599D+02	9.6527D+01	1.8925D+01	6.4436D+01	6.7436D-01	0.0000D+00
13	2.5069D+02	1.1877D+02	2.0000D+01	6.0972D+01	9.1284D+00	0.0000D+00
14	3.1496D+02	1.1983D+03	1.4793D+00	0.0000D+00	9.1284D+00	1.0000D+00
15	3.1638D+02	2.8651D+02	4.0000D+02	0.0000D+00	0.0000D+00	0.0000D+00
16	3.1088D+02	2.8087D+02	4.0000D+02	0.0000D+00	0.0000D+00	0.0000D+00
17	2.8877D+02	1.4597D+02	3.6214D+01	6.7346D+01	9.1284D+00	0.0000D+00
18	2.8509D+02	1.3350D+02	2.0277D+01	6.0140D+01	9.1284D+00	0.0000D+00
19	1.8894D+02	1.5693D+02	1.4793D+00	0.0000D+00	9.1284D+00	0.0000D+00
20	1.8894D+02	1.1416D+03	1.4793D+00	0.0000D+00	9.1284D+00	1.0000D+00
21	3.9366D+01	1.5693D+02	1.4793D+00	0.0000D+00	1.1874D-01	1.3941D-01
22	8.8923D+01	5.6790D+01	1.0753D+00	0.0000D+00	6.7436D-01	0.0000D+00
23	8.5000D+01	5.2890D+01	3.9100D+02	0.0000D+00	0.0000D+00	0.0000D+00
24	8.8006D+01	5.5878D+01	3.9100D+02	0.0000D+00	0.0000D+00	0.0000D+00
25	8.8923D+01	1.0997D+03	1.0753D+00	0.0000D+00	6.7436D-01	1.0000D+00
26	3.9366D+01	5.6790D+01	1.0753D+00	0.0000D+00	1.1874D-01	4.5870D-02
27	3.9366D+01	1.9717D+02	4.8613D+00	0.0000D+00	1.1874D-01	1.7699D-01
28	5.9432D+01	2.7525D+01	3.0000D+02	0.0000D+00	0.0000D+00	0.0000D+00
29	4.5000D+01	1.3247D+01	3.0000D+02	0.0000D+00	0.0000D+00	0.0000D+00
30	3.9366D+01	1.9717D+02	4.8613D+00	0.0000D+00	1.1874D-01	1.7699D-01
31	1.7022D+02	8.1525D+01	2.0108D+01	6.0644D+01	6.7436D-01	0.0000D+00
32	3.1496D+02	1.5436D+02	1.8521D+01	6.5842D+01	9.1284D+00	0.0000D+00
33	4.3983D+02	2.0497D+02	2.0000D+01	6.0972D+01	8.7427D+01	0.0000D+00
34	4.4083D+02	2.0542D+02	2.0009D+01	6.0946D+01	8.7427D+01	0.0000D+00
35	5.0000D+02	4.7713D+02	4.1600D+02	0.0000D+00	0.0000D+00	0.0000D+00
36	4.9319D+02	4.6998D+02	4.1600D+02	0.0000D+00	0.0000D+00	0.0000D+00
37	4.9951D+02	2.3462D+02	1.7693D+01	6.8921D+01	8.7427D+01	0.0000D+00
38	4.9951D+02	1.2663D+03	2.3068D+00	0.0000D+00	8.7427D+01	1.0000D+00
39	3.1824D+02	1.1847D+03	2.3068D+00	0.0000D+00	8.7427D+01	1.0000D+00
40	3.1824D+02	2.8842D+02	2.3068D+00	0.0000D+00	8.7427D+01	0.0000D+00
41	3.9366D+01	2.8842D+02	2.3068D+00	0.0000D+00	1.1874D-01	2.6222D-01
42	2.5069D+02	1.1877D+02	2.0000D+01	6.0972D+01	9.1284D+00	0.0000D+00
43	1.5618D+02	7.5788D+01	4.0000D+01	6.0972D+01	6.7436D-01	0.0000D+00
44	2.5069D+02	1.1877D+02	4.0000D+01	6.0972D+01	9.1284D+00	0.0000D+00
45	1.7429D+02	9.8490D+01	3.6214D+01	6.7346D+01	6.7436D-01	0.0000D+00
46	2.5983D+02	1.3719D+02	1.7693D+01	6.8921D+01	9.1284D+00	0.0000D+00
47	1.5618D+02	7.5788D+01	6.0000D+01	6.0972D+01	6.7436D-01	0.0000D+00

Equivalent Unit Heat Transfer Characteristics for Each Unit

No.	Type	UA	EFF	CAT	LMTD
1	Evaporator	3.7700D+02	7.1923D-01	5.6340D+00	1.1362D+01
2	Absorber	1.9300D+02	4.0661D-01	2.8303D+01	3.1545D+01
3	Desorber	2.6800D+02	9.0229D-01	1.7079D+00	5.7478D+00
4	Desorber	2.6800D+02	9.5443D-01	1.4261D+00	8.4173D+00
5	Condenser	5.6500D+02	7.6629D-01	9.1679D-01	2.0679D+00
6	Condenser	5.6500D+02	7.5385D-01	1.2479D+00	2.7264D+00
7	Heat Exger	6.4000D+01	7.7414D-01	1.4730D+01	1.8269D+01
8	Heat Exger	6.4000D+01	8.6344D-01	1.8106D+01	2.6867D+01
9	Mixer	0.0000D+00	0.0000D+00	0.0000D+00	0.0000D+00
10	Valve	0.0000D+00	0.0000D+00	0.0000D+00	0.0000D+00
11	Valve	0.0000D+00	0.0000D+00	0.0000D+00	0.0000D+00
12	Heat Exger	6.4000D+01	9.6327D-01	9.1397D+00	2.6935D+01
13	Desorber	2.6800D+02	9.9176D-01	4.8780D-01	1.1093D+01
14	Condenser	5.6500D+02	7.4788D-01	1.8545D+00	3.9926D+00
15	Valve	0.0000D+00	0.0000D+00	0.0000D+00	0.0000D+00
16	Mixer	0.0000D+00	0.0000D+00	0.0000D+00	0.0000D+00

17	Mixer	0.0000D+00	0.0000D+00	0.0000D+00	0.0000D+00
18	Splitter	0.0000D+00	0.0000D+00	0.0000D+00	0.0000D+00
19	Splitter	0.0000D+00	0.0000D+00	0.0000D+00	0.0000D+00

No.	Type	Heat Transfer	Eq. Dev.	IPInch
1	Evaporator	4.2835D+03	0.000D+00	-1
2	Absorber	6.0882D+03	0.000D+00	-1
3	Desorber	1.5404D+03	0.000D+00	1
4	Desorber	2.2558D+03	0.000D+00	1
5	Condenser	1.1683D+03	0.000D+00	1
6	Condenser	1.5404D+03	0.000D+00	1
7	Heat Exger	1.1692D+03	0.000D+00	-1
8	Heat Exger	1.7195D+03	0.000D+00	-1
9	Mixer	0.0000D+00	0.000D+00	0
10	Valve	0.0000D+00	0.000D+00	0
11	Valve	0.0000D+00	0.000D+00	0
12	Heat Exger	1.7239D+03	0.000D+00	-1
13	Desorber	2.9731D+03	0.000D+00	1
14	Condenser	2.2558D+03	0.000D+00	1
15	Valve	0.0000D+00	0.000D+00	0
16	Mixer	0.0000D+00	0.000D+00	0
17	Mixer	0.0000D+00	0.000D+00	0
18	Splitter	0.0000D+00	0.000D+00	0
19	Splitter	0.0000D+00	0.000D+00	0

COP = 1.4408

Table A-3. NH₃-H₂O 1-Effect Chiller with Rectifier, Desorber/Mixer, and Precooler

State Point	Temper.	Enthalpy	Flow Rate	Concentr.	Pressure	Vapor Fr.
1	6.0000D+01	2.8087D+01	4.7940D+01	0.0000D+00	0.0000D+00	0.0000D+00
2	5.6179D+01	2.4304D+01	4.7940D+01	0.0000D+00	0.0000D+00	0.0000D+00
3	4.2986D+01	5.5246D+02	3.5000D-01	9.9960D+01	5.2531D+01	9.9974D -01
4	8.5000D+01	5.2890D+01	9.0600D+00	0.0000D+00	0.0000D+00	0.0000D+00
5	1.1456D+02	8.2324D+01	9.0600D+00	0.0000D+00	0.0000D+00	0.0000D+00
6	9.5664D+01	-4.1460D+01	3.0000D+00	4.5597D+01	5.2531D+01	0.0000D+00
7	1.7124D+02	4.1616D+01	3.0000D+00	4.5597D+01	1.6945D+02	0.0000D+00
8	2.2000D+02	1.8830D+02	9.6400D+00	0.0000D+00	0.0000D+00	0.0000D+00
9	1.8838D+02	1.5636D+02	9.6400D+00	0.0000D+00	0.0000D+00	0.0000D+00
10	9.0564D+01	5.5792D+02	3.5000D-01	9.9960D+01	1.6945D+02	1.0000D+00
11	1.9462D+02	7.1254D+01	2.6500D+00	3.8417D+01	1.6945D+02	0.0000D+00
12	1.1070D+02	-2.2794D+01	2.6500D+00	3.8417D+01	5.2531D+01	0.0000D+00
13	8.5000D+01	5.2890D+01	4.8460D+01	0.0000D+00	0.0000D+00	0.0000D+00
14	8.8611D+01	5.6480D+01	4.8460D+01	0.0000D+00	0.0000D+00	0.0000D+00
15	8.6200D+01	6.0922D+01	3.5000D-01	9.9960D+01	1.6945D+02	0.0000D+00
16	1.1701D+02	-1.6557D+01	2.6777D+00	3.9055D+01	5.2531D+01	0.0000D+00
17	1.7074D+02	4.1070D+01	3.0242D+00	4.5463D+01	1.6945D+02	0.0000D+00
18	2.3827D+01	3.4250D+01	3.5000D-01	9.9960D+01	5.2531D+01	7.8727D-02
19	9.0564D+01	5.5792D+02	3.5000D-01	9.9960D+01	1.6945D+02	1.0000D+00
20	2.3827D+01	3.4250D+01	3.5000D-01	9.9960D+01	5.2531D+01	7.8727D-02
21	1.7147D+02	4.1892D+01	3.0283D+00	4.5530D+01	1.6945D+02	0.0000D+00
22	1.9462D+02	7.1254D+01	2.8271D-02	3.8417D+01	1.6945D+02	0.0000D+00
23	1.9462D+02	6.5031D+02	3.7827D-01	9.5360D+01	1.6945D+02	1.0000D+00
24	8.5000D+01	5.2890D+01	6.0000D-01	0.0000D+00	0.0000D+00	0.0000D+00
25	1.6623D+02	1.3407D+02	6.0000D-01	0.0000D+00	0.0000D+00	0.0000D+00
26	1.9462D+02	6.5031D+02	3.7827D-01	9.5360D+01	1.6945D+02	1.0000D+00

27	4.2986D+01	-6.6955D+01	8.0008D-05	7.2334D+01	5.2531D+01	0.0000D+00
28	4.2986D+01	5.5260D+02	3.4992D-01	9.9966D+01	5.2531D+01	1.0000D+00
29	6.2634D+01	3.4250D+01	3.5000D-01	9.9960D+01	1.6945D+02	0.0000D+00
30	8.6164D+01	5.7913D+02	3.5000D-01	9.9960D+01	5.2531D+01	1.0000D+00

Equivalent Unit Heat Transfer Characteristics for Each Unit

No.	Type	UA	EFF	CAT	LMTD
1	Desorber	7.5992D+00	5.2965D-01	1.7014D+01	2.3867D+01
2	Heat Exger	1.3186D+01	8.4805D-01	1.5036D+01	1.8901D+01
3	Desorber	1.4475D+01	6.4198D-01	1.7637D+01	2.1275D+01
4	Condenser	1.1251D+02	7.8439D-01	1.1998D+00	1.5461D+00
5	Absorber	4.7724D+01	9.2335D-01	2.4534D+00	5.5878D+00
6	Valve	0.0000D+00	0.0000D+00	0.0000D+00	0.0000D+00
7	Rectifier	8.1010D-01	7.4102D-01	2.8389D+01	6.0125D+01
8	Mixer	0.0000D+00	0.0000D+00	0.0000D+00	0.0000D+00
9	Mixer	0.0000D+00	0.0000D+00	0.0000D+00	0.0000D+00
10	Heat Exger	3.0024D+00	9.9917D-01	3.5809D-02	3.1093D+00

No.	Type	Heat Transfer	Eq. Dev.	IPInch
1	Desorber	1.8137D+02	0.000D+00	1
2	Heat Exger	2.4923D+02	0.000D+00	-1
3	Desorber	3.0796D+02	0.000D+00	-1
4	Condenser	1.7395D+02	0.000D+00	-1
5	Absorber	2.6667D+02	0.000D+00	1
6	Valve	0.0000D+00	0.000D+00	0
7	Rectifier	4.8707D+01	0.000D+00	1
8	Mixer	0.0000D+00	0.000D+00	0
9	Mixer	0.0000D+00	0.000D+00	0
10	Heat Exger	9.3354D+00	0.000D+00	1

COP = .5890

Table A-4. NH₃-H₂O Generator-Absorber Heat Exchanger, Phillips Cooling Mode

State Point	Temper.	Enthalpy	Flow Rate	Concentr.	Pressure	Vapor Fr.
1	0.0000D+00	-3.1090D+01	0.0000D+00	0.0000D+00	0.0000D+00	0.0000D+00
2	0.0000D+00	-3.1090D+01	0.0000D+00	0.0000D+00	0.0000D+00	0.0000D+00
3	4.8000D+01	5.1379D+02	1.0000D+00	9.9539D+01	8.0300D+01	9.3532D-01
4	2.2923D+02	1.9766D+02	1.4000D+01	0.0000D+00	0.0000D+00	0.0000D+00
5	2.4364D+02	2.1227D+02	1.4000D+01	0.0000D+00	0.0000D+00	0.0000D+00
6	2.7765D+02	1.7887D+02	1.4963D+00	2.7292D+01	2.7740D+02	0.0000D+00
7	0.0000D+00	-3.1090D+01	0.0000D+00	0.0000D+00	0.0000D+00	0.0000D+00
8	0.0000D+00	-3.1090D+01	0.0000D+00	0.0000D+00	0.0000D+00	0.0000D+00
9	0.0000D+00	-3.1090D+01	0.0000D+00	0.0000D+00	0.0000D+00	0.0000D+00
10	1.5100D+02	5.8591D+02	1.0000D+00	9.9539D+01	2.7740D+02	1.0000D+00
11	2.3616D+02	1.2068D+02	1.7004D+00	3.7446D+01	2.7740D+02	0.0000D+00
12	2.7765D+02	7.4436D+02	4.5966D-01	8.4489D+01	2.7740D+02	1.0000D+00
13	0.0000D+00	-3.1090D+01	0.0000D+00	0.0000D+00	0.0000D+00	0.0000D+00
14	0.0000D+00	-3.1090D+01	0.0000D+00	0.0000D+00	0.0000D+00	0.0000D+00
15	1.0803D+02	8.5333D+01	1.0000D+00	9.9539D+01	2.7740D+02	0.0000D+00
16	2.8228D+02	2.3424D+02	1.0926D+00	5.5449D+00	8.0300D+01	0.0000D+00

17	2.7765D+02	1.7887D+02	1.4963D+00	2.7292D+01	2.7740D+02	0.0000D+00
18	4.4815D+01	2.1939D+01	1.0000D+00	9.9539D+01	8.0300D+01	1.7415D-02
19	1.5100D+02	5.8591D+02	1.0000D+00	9.9539D+01	2.7740D+02	1.0000D+00
20	4.4815D+01	2.1939D+01	1.0000D+00	9.9539D+01	8.0300D+01	1.7415D-02
21	2.2289D+02	1.0358D+02	2.0889D+00	4.9796D+01	2.7740D+02	0.0000D+00
22	2.0129D+02	7.7464D+01	5.2232D-02	4.7474D+01	2.7740D+02	0.0000D+00
23	2.0129D+02	6.3383D+02	1.0522D+00	9.6955D+01	2.7740D+02	1.0000D+00
24	0.0000D+00	-3.1090D+01	0.0000D+00	0.0000D+00	0.0000D+00	0.0000D+00
25	0.0000D+00	-3.1090D+01	0.0000D+00	0.0000D+00	0.0000D+00	0.0000D+00
26	2.0129D+02	6.3383D+02	1.0522D+00	9.6955D+01	2.7740D+02	1.0000D+00
27	4.8000D+01	-5.9639D+00	6.2097D-02	9.2712D+01	8.0300D+01	0.0000D+00
28	4.8000D+01	5.4820D+02	9.3790D-01	9.9991D+01	8.0300D+01	1.0000D+00
29	5.3097D+01	2.1939D+01	1.0000D+00	9.9539D+01	2.7740D+02	0.0000D+00
30	9.5000D+01	5.7718D+02	1.0000D+00	9.9539D+01	8.0300D+01	9.9523D-01
31	2.3301D+02	1.5499D+02	1.2808D+00	1.5395D+01	8.0300D+01	0.0000D+00
32	2.3301D+02	7.8171D+02	2.4417D-01	7.2563D+01	8.0300D+01	1.0000D+00
33	1.0800D+02	-2.6422D+01	2.0367D+00	4.9856D+01	8.0300D+01	0.0000D+00
34	2.2351D+02	1.0425D+02	2.0367D+00	4.9856D+01	8.0300D+01	0.0000D+00
35	2.3301D+02	1.5499D+02	1.2808D+00	1.5395D+01	8.0300D+01	0.0000D+00
36	2.4237D+02	2.0471D+02	1.0367D+00	1.9303D+00	2.7740D+02	0.0000D+00
37	4.0000D+02	3.7014D+02	1.0367D+00	1.9303D+00	2.7740D+02	0.0000D+00
38	1.6533D+02	4.3527D+01	1.5445D+00	3.2568D+01	8.0300D+01	0.0000D+00
39	1.6533D+02	6.4141D+02	5.0779D-01	9.5118D+01	8.0300D+01	1.0000D+00
40	1.6533D+02	4.3527D+01	1.5445D+00	3.2568D+01	8.0300D+01	0.0000D+00
41	0.0000D+00	-3.1090D+01	0.0000D+00	0.0000D+00	0.0000D+00	0.0000D+00
42	2.3616D+02	1.2068D+02	1.7004D+00	3.7446D+01	2.7740D+02	0.0000D+00
43	2.3616D+02	6.7982D+02	6.6371D-01	9.2920D+01	2.7740D+02	1.0000D+00
44	2.0129D+02	7.7464D+01	1.9909D+00	4.7474D+01	2.7740D+02	0.0000D+00

Equivalent Unit Heat Transfer Characteristics for Each Unit

No.	Type	UA	EFF	CAT	LMTD
1	Desorber	0.0000D+00	0.0000D+00	0.0000D+00	0.0000D+00
2	Analyzer	4.4000D+00	9.6205D-01	6.2172D+00	3.8977D+01
3	Desorber	0.0000D+00	0.0000D+00	0.0000D+00	0.0000D+00
4	Condenser	0.0000D+00	0.0000D+00	0.0000D+00	0.0000D+00
5	Absorber	1.3643D+01	9.2879D-01	3.7777D+00	1.4995D+01
6	Valve	0.0000D+00	0.0000D+00	0.0000D+00	0.0000D+00
7	Rectifier	0.0000D+00	0.0000D+00	0.0000D+00	0.0000D+00
8	Mixer	0.0000D+00	0.0000D+00	0.0000D+00	0.0000D+00
9	Mixer	0.0000D+00	0.0000D+00	0.0000D+00	0.0000D+00
10	Heat Exger	7.5000D+00	9.1509D-01	5.0975D+00	8.4526D+00
11	Analyzer	1.0000D+01	9.2398D-01	9.5032D+00	2.6613D+01
12	Analyzer	0.0000D+00	0.0000D+00	0.0000D+00	0.0000D+00
13	Analyzer	1.3178D+01	8.2338D-01	7.4782D+00	1.5524D+01

No.	Type	Heat Transfer	Eq. Dev.	IPInch
1	Desorber	4.9185D+02	0.000D+00	1
2	Analyzer	1.7150D+02	0.000D+00	-1
3	Desorber	4.5823D+02	0.000D+00	-1
4	Condenser	5.0058D+02	-9.900D+00	-1
5	Absorber	2.0457D+02	0.000D+00	-1
6	Valve	0.0000D+00	0.000D+00	0
7	Rectifier	7.6979D+01	0.000D+00	1
8	Mixer	0.0000D+00	0.000D+00	0
9	Mixer	0.0000D+00	0.000D+00	0
10	Heat Exger	6.3394D+01	0.000D+00	-1
11	Analyzer	2.6613D+02	0.000D+00	1

12 Analyzer	3.7252D+02	0.000D+00	0
13 Analyzer	2.0457D+02	0.000D+00	1

COP = 1.0734

**Enhanced Absorption Cycle Computer Model
Appendix B
Users' Manual**

APPENDIX B USERS' MANUAL

This manual describes in detail the parameters required on each card of the input, their mathematical symbols, and their formats.

B.1. GENERAL INFORMATION

The first card allows the user to supply a problem title. If no title is desired, input "blanks." The card has the following format:

Title card	Columns	1	2-66 <i>ATITLE</i>
	Format	1X	A65
Explanation			
<i>ATITLE</i>		Name or title of problem, which can consist of any characters	

The second card includes scaling parameters for normalization and has the following format:

Scaling parameter card	Columns	1-10 <i>TMAX</i>	11-20 <i>TMIN</i>	21-30 <i>FMAX</i>	31-40 <i>PMAX</i>
	Format	F10.1	F10.1	F10.1	F10.1
Explanation					
<i>TMAX</i>		maximum expected temperature in the system			
<i>TMIN</i>		minimum expected temperature in the system			
<i>FMAX</i>		maximum expected mass flow rate in the system			
<i>PMAX</i>		maximum expected pressure in the system			

The third card contains control parameters and has the following format:

Control card	Columns	1-5 <i>MAXFEV</i>	6-10 <i>MSGLVL</i>	11-15 <i>IUFLAG</i>	16-25 <i>FTOL</i>	26-35 <i>XTOL</i>	36-40 <i>NEWDAT</i>
	Format	I5	I5	I5	D10.1	D10.1	I5
Explanation							
<i>MAXFEV</i>	maximum number of iterations allowed before termination						
<i>MSGLVL</i>	integer flag controlling the printing of intermediate results						
= 0	no intermediate results are printed						
= <i>n</i>	intermediate results are printed every <i>n</i> iterations						
<i>IUFLAG</i>	integer flag indicating the system of units used for the input and final output results (intermediate results are always in British units)						
= 1	input and output in British units						
= 2	input in British units; output in SI units						
= 3	input and output in SI units						
= 4	input in SI units; output in British units						
<i>FTOL</i>	Convergence tolerance on the value of the functions' residuals. Exit from the solver routine occurs when the Euclidian norm of the residuals is less than <i>FTOL</i> .						
> 0							
<i>XTOL</i>	Convergence tolerance on the values of the variables. Exit from the solver routine occurs when the relative error between two successive iterations is at most <i>XTOL</i> .						
> 0							
<i>NEWDAT</i>	integer flag controlling the generation of an optional new input file <i>NEW.DAT</i> based on the results of the current run						
= 0	new input file is not generated						
> 0	new input file is generated						

The fourth card indicates the number of units and state points in the system and has the following format:

System card	Columns	1-4 <i>NUNITS</i>	5-8 <i>NSP</i>
	Format	I4	I4
Explanation			
<i>NUNITS</i>		total number of units or components	
<i>NSP</i>		total number of state points	

B.2. USER INPUT

This part of the input describes the units that compose the system. The user must supply two data cards for each unit. The first card provides a unit description and has the following format:

Unit I.D. card	Columns	1-5 <i>NU</i>	6-10 <i>IDUNIT</i>	11-15 <i>IHT</i>	16-25 <i>HT</i>	26-30 <i>IPINCH</i>	31-40 <i>DEV</i>	41-45 <i>ICOP</i>
	Format	I5	I5	I5	F10.4	I5	F10.4	I5
	Explanation							
	<i>NU</i>	number assigned to the unit in the cycle diagram						
	<i>IDUNIT</i>	Unit type: = 1 Absorber = 2 Desorber = 3 Heat Exchanger = 4 Condenser = 5 Evaporator = 6 Valve = 7 Mixer = 8 Splitter = 9 Rectifier = 10 Analyser = 11 Compressor = 12 Pump						
	<i>IHT</i>	integer index indicating method of specification of unit heat transfer characteristics = 1 <i>UA</i> Method = 2 <i>EFF</i> Method = 3 <i>CAT</i> Method = 4 <i>LMTD</i> Method						
	<i>HT</i>	value of <i>UA</i> or <i>EFF</i> or <i>CAT</i> or <i>LMTD</i> according to <i>IHT</i> index						
	<i>IPINCH</i>	integer index indicating location of temperature pinch = -1 pinch at cold end = +1 pinch at hot end = 0 program decides the location of the pinch						
	<i>DEV</i>	temperature deviation from the equilibrium state						
	<i>ICOP</i>	integer index for calculating coefficient of performance based on the heat duty of the current unit = +1 heat duty of current unit added to COP numerator = -1 heat duty of current unit added to COP denominator = 0 heat duty of current unit not included in COP calculation						

The second card describes how the unit is connected to other units in the system. The user must list the numbers of the state points associated with the unit in the system in an order corresponding to that in the unit subroutine. The card has the following format:

State point order card	Columns	1-4 ISP-1	5-8 ISP-2	9-12 ISP-3	13-16 ISP-4	17-20 ISP-5	21-24 ISP-6	25-28 ISP-7
	Format	I4	I4	I4	I4	I4	I4	I4
Explanation								
<i>ISP</i>		state point number to be listed in the order 1 to 7, corresponding with the unit subroutine						

B.3. STATE POINT INPUT

This part of the input requires one card for each state point in the cycle. The card gives the state point number, a code for the working fluid in it, and five pairs of numbers for the temperature, mass flow rate, concentration, pressure, and vapor fraction at that state point. In each pair of numbers, the first is an integer indicating a fixed or variable quantity, and the second is a real number giving a fixed value or an initial guess for the quantity in question.

The user must supply for each state point one input card that has the following format:

Initial values card	Columns	1-5 <i>NDUM</i>	6-10 <i>KSUB</i>	11-14 <i>ITFIX</i>	15-20 <i>T</i>	21-24 <i>IFFIX</i>	25-30 <i>F</i>
	Format	I5	I5	I4	F6.1	I4	F6.1
	Columns	31-34 <i>ICFIX</i>	35-40 <i>C</i>	41-44 <i>IPFIX</i>	45-50 <i>P</i>	51-54 <i>IWFIX</i>	55-60 <i>W</i>
	Format	I4	F6.1	I4	F6.1	I4	F6.1
Explanation							
<i>NDUM</i>	state point number in the cycle diagram						
<i>KSUB</i>	type of working fluid						
= 1	LiBr-H ₂ O		solution				
= 2	H ₂ O-NH ₃		solution and vapor				
= 3	H ₂ O		liquid and vapor				
= 4	LiBr-H ₂ O-NH ₃		solution				
= 5	LiBr/ZnBr ₂ -CH ₃ OH		solution				
= 6	CH ₃ OH		liquid and vapor				
= 7	LiNO ₃ /KNO ₃ /NaNO ₃ -H ₂ O		solution				
= 8	NaOH-H ₂ O		solution				
= 9	LiCl-H ₂ O		solution				
<i>ITFIX</i>	integer index for temperature						
= 0	fixed temperature						
= 1	variable temperature, not equal to the temperature at any other state point						
≥ 2	Variable temp. State points for which this integer is the same have identical temperatures.						
<i>T</i>	initial value of temperature						
<i>IFFIX</i>	same as <i>ITFIX</i> , for mass flow rate instead of temperature						
<i>F</i>	initial value of mass flow rate						
<i>ICFIX</i>	same as <i>ITFIX</i> , for concentration instead of temperature						

<i>C</i>	initial value of concentration
<i>IPFIX</i>	same as <i>ITFIX</i> , for pressure instead of temperature
<i>P</i>	initial value of pressure
<i>IWFIX</i>	same as <i>ITFIX</i> , for vapor fraction instead of temperature
<i>W</i>	initial value of vapor fraction

INTERNAL DISTRIBUTION

- | | | | |
|-----|-----------------|--------|----------------------------------|
| 1. | M. R. Ally | 18. | W. R. Mixon |
| 2. | K. J. Ballew | 19. | R. W. Murphy |
| 3. | V. D. Baxter | 20. | D. E. Reichle |
| 4. | R. S. Carlsmith | 21. | R. H. Reiner |
| 5. | F. C. Chen | 22. | C. K. Rice |
| 6. | D. M. Counce | 23. | M. W. Rosenthal |
| 7. | G. E. Courville | 24. | J. R. Sand |
| 8. | F. A. Creswick | 25. | R. B. Shelton |
| 9. | R. C. DeVault | 26. | J. A. Shonder |
| 10. | P. D. Fairchild | 27. | E. A. Vineyard |
| 11. | S. K. Fischer | 28. | W. R. Wilburn |
| 12. | W. Fulkerson | 29. | A. Zaltash |
| 13. | P. J. Hughes | 30-31. | Laboratory Records
Department |
| 14. | M. A. Kuliasha | 32. | Laboratory Records-RC |
| 15. | W. P. Levins | 33. | ORNL Patent Office |
| 16. | V. C. Mei | 34. | Central Research Library |
| 17. | W. A. Miller | 35. | Document Reference Section |

EXTERNAL DISTRIBUTION

36. G. Alefeld, Physik-Department, Technische Universitat Munchen, James-Franck-Strasse, D-8046 Garching b. Munchen, Federal Republic of Germany
37. D. A. Ball, Battelle Columbus Laboratories, 505 King Avenue, Columbus, OH 43201-2693
38. J. Bassols, Rendamax BV, Hamstraat 76, P.O. Box 1035, 6460 BA Kerkrade, The Netherlands
39. F. Bawel, 744 E. Tennyson Rd., Boonville, TN 47601
40. E. W. Becker, M. L. 19EO, Southern California Gas Company, Box 3249, Los Angeles, CA 90051-1249
41. M. Behar, Agence Francaise pour la Maitrise, de l'Energie, Route des Lucioles, 06565 Valbonne Cedex, France
42. J. Berghmans, Universiteit Leuven, Instituut Mechanica, Celestynen Laan 300A, B-3030 Heverlee, Belgium

43. T. Berntsson, Chalmers University of Technology, S-41296 Gothenburg, Sweden
44. W. J. Biermann, 45 Foxcroft Drive, Fayetteville, NY 13066
45. D. R. Bohi, Energy and Natural Resources Division, Resources for the Future, 1616 P Street, N.W., Washington, D.C. 20036
46. U. Bonne, Honeywell Corporate Technology Center, 10701 Lyndale Avenue South, Boomington, MN 55420
47. I. Borde, The Institutes for Applied Research, Ben-Gurion University of the Negev, P.O. Box 1025, Beer-Sheva 84110, Israel
48. M. Boulanger, Centre de Recherche Industrielle du Quebec, 333, rue Franquet, Case postale 9038, Sainte-Foy (Quebec) Canada G1V 4C7
49. J. W. J. Bouma, Novem, Postbus 17, 6130 AA Sittard, The Netherlands
50. R. Bugarel, Institut de Genie Chimique, Chemin de la Loge, Toulouse Cedex, France
51. J. M. Calm, Engineering Consultant, 10887 Woodleaf Lane, Great Falls, VA 22066
52. J. Cheron, Direction de Recherche, Physico-chimie appliquee et analyse, Institut Francais du Petrole, 1 and 4 avenue de Bois-Preau BP 311, 92506 Rueil Malmaison Cedex, France
53. R. N. Christensen, Ohio State University, 206 West 18th Ave., Columbus, OH 43210-1107
54. R. Cohen, Ray W. Herrick Laboratories, Purdue University, West Lafayette, IN 47907
55. A. T. Conlisk, Ohio State University, 206 West 18th Ave., Columubs, OH 43210-1107
56. D. D. Colosimo, Mechanical Technology, Inc., 968 Albany-Shaker Road, Latham, NY 12110
57. P. O. Danig, Technical University of Denmark, Refrigeration Laboratory, DTH 402B, DK-2800 Lyngby, Denmark

58. K. Dao, Research & Development, RA Technology, 12 Nace Ave., Piedmont, CA 94611
59. K. Davidson, Gas Research Institute, 8600 West Bryn Mawr Avenue, Chicago, IL 60631
60. A. C. DeVuono, Battelle, Columbus Division, 505 King Avenue, Columbus, OH 43201-2693
61. D. A. Didion, National Institute of Standards & Technology, CBT, Gaithersburg, MD 20899
62. W. Dolan, Gas Research Institute, 8600 West Bryn Mawr Avenue, Chicago, IL 60631
63. T. E. Drabek, Department of Sociology, University of Denver, Denver, CO 80208-0209
64. D. D'Zhurko, New York Gas Group, 500 Fifth Ave., Suite 428, New York, NY 10110
65. J. Engelhard, M.A.N., Neue Technologie, Dachauer Strasse 667, 8000 München 50, Federal Republic of Germany
66. D. C. Erickson, Energy Concepts Co., 627 Ridgely Ave., Annapolis, MD 21401
67. M. Falek, York International, P.O. Box 1592, York, PA 17405-1592
68. R. J. Fiskum, CE-422, 5H-048/FORSTAL, U.S. Department of Energy, 1000 Independence Avenue, SW, Washington, DC 20585
69. S. Freedman, Gas Research Institute, 8600 West Bryn Mawr Avenue, Chicago, IL 60631
70. P. E. Frivik, SINTEF-N.TH., Division Refr. Eng., N-7034 Trondheim, Norway
71. B. Genest, Direction des Etudes et de Recherches Nouvelles, Centre D'Essais et des Recherches sur les Utilisations du Gaz, Gaz de France, 361 Avenue du President Wilson BP 33, 93211 LaPlaine Saint-Denis Cedex, France
72. T. Gilles, Lennox Industries Incorporated, P.O. Box 799900, Dallas, TX 75379-9900

73. P. Glamm, The Trane Company, 3600 Pammel Creek Road, LaCrosse, WI 54601-7599
74. E. Granryd, Royal Institute of Technology, Department of Applied Thermodynamics and Refrigeration, S-100-44 Stockholm, Sweden
- 75-79. G. Grossman, Technion Institute of Technology, Faculty of Mechanical Engineering, Haifa 32000, Israel
80. M. E. Gunn, CE-12, 5F-043/FORSTAL, U.S. Department of Energy, 1000 Independence Avenue, SW, Washington, DC 20585
81. H. Hale, United Technologies Carrier, A&R Building, Carrier Parkway, Syracuse, NY 13221
82. H. Halozan, Graz University of Technology, Inffeldgasse 25, A-8010 Graz, Austria
83. W. T. Hanna, Battelle Columbus Laboratories, 505 King Avenue, Columbus, OH 43201-2693
84. P. Hay, PLE-PBE, KFA-Jülich GmbH, Postfach 1913, D-5170 Jülich, Federal Republic of Germany
85. K. Herold, Center for Environmental Energy Engineering, University of Maryland, College Park, MD 20742
86. S. J. Hemmelgarn, The ARCTEK Corporation, 1 Century Drive, Gettysburg, OH 45328
87. K. E. Hickman, York International Corporation, P.O. Box 1592-191A, York, PA 17405-1592
88. D. L. Hodgett, Chemical & Process Industries Division, Electricity Research & Development Centre, Capenhurst Chester, UK CH1 6ES
89. K. Holzapfel, Joseph Haydn Str. 29, D-7524 Ostringen, Federal Republic of Germany
90. P. Iedema, FDO Technische Adviseurs, P.O. Box 194, 7550 AD Hengelo, The Netherlands
91. Y. Igarashi, Heat Pump Technology Center of Japan, Asuma-Shurui Bldg. 2-9-11, Kanda-Awajicho, Chiyoda-ku, Tokyo 100, Japan

92. T. Ikepa, Angel Research Inc., 13740 Omega Road, Dallas, TX 75244-4516
93. N. Inoue, Ebara Corporation, Refrigeration Products & Systems Division, 2-1 Hon Fujisawa 4-chome, Fujisawa-shi 251, Japan
94. F. E. Irwin, United Technologies Carrier, 6376 Wavel St., Syracuse, NY 13026
95. N. Isshiki, Nihon University, Koriyama 963, Japan
96. P. Joyner, Electric Power Research Institute, P.O. Box 10412, Palo Alto, CA 94303
97. T. Kapus, Building Equipment Division, CE-422, 5H-048/FORSTAL, U.S. Department of Energy, 1000 Independence Avenue, SW, Washington, DC 20585
98. T. Kashiwagi, Dept. of Mech. Systems Engrg., Tokyo University of Agriculture & Technology, 24-16, Nakamachi 2-chome, Koganei, Tokyo 184, Japan
99. J. U. Keller, Institut für Fluid-und-Thermodynamik, Universität Silgen, Postfach 101240, 5900 Siegen, Federal Republic of Germany
100. S. A. Klein, University of Wisconsin, Mechanical Engineering Department, Madison, WI 53706
101. K. F. Knoche, Lehrstuhl für Technische Thermodynamik, RWTH Aachen, Schinkelstrasse 8, 5100 Aachen, Federal Republic of Germany
102. J. Kohler, York International, P. O. Box 1592, York, PA 17405-1592
103. D. Kuhlenschmidt, The ARCTEK Corporation, 1 Century Drive, Gettysburg, OH 45328
104. A. Lannus, Electric Power Research Institute, P.O. Box 10412, Palo Alto, CA 94303
105. M. A. Laudau, M. L. 19EO, Southern California Gas Company, Box 3249, Los Angeles, CA 90051-1249
106. H. J. Laue, Leiter Informationszentrum Wärmepumpen und Kältetechnik, Fachinformationszentrum Karlsruhe GmbH, D-7514 Eggenstein-Leopoldshafen 2, Germany

107. Z. Lavan, Department of Mechanical Engineering, Illinois Institute of Technology, Chicago, IL 60616
108. P. LeGoff, Laboratoire des Sciences du Genie Chimique, CNRS-ENSIC-INPL-Nancy, France
109. J. G. Liggett, The ARCTEK Corporation, 1 Century Drive, Gettysburg, OH 45328
110. I. R. G. Lowe, NRC-Canada, Bldg. R.105, Montreal Rd., Ottawa K1A 0R6 Canada
111. C. D. MacCracken, Calmac Manufacturing Corporation, 101 West Sheffield Avenue, P.O. Box 710, Englewood, NJ 07631
112. R. A. Macriss, 1603 Oak Terrace, St. Joseph, MI 49085
113. W. Malewski, Borsig GmbH, Berlinerstr. 27/33, D-1000 Berlin, Federal Republic of Germany
114. J. Marsala, Gas Research Institute, 8600 West Byrn Mawr Ave., Chicago, IL 60631
115. K. R. McGahey, Ohio State University, 206 West 18th Ave., Columbus, OH 43210-1107
116. L. A. McNeely, 7310 Steinmeier Drive, Indianapolis, IN 46250
117. G. Melikian, United Technology Research Center, 411 Silver Lane, East Hartford, CT 06108
118. M. S. Menzer, Air Conditioning & Refrigeration Institute, 1501 Wilson Blvd., Arlington, VA 22209
119. F. Meunier, Laboratoire de Thermodynamique des Fluides, CNRS, Campus Universitaire-Bat 502 Ter., 91405 Orsay Cedex, France
120. J. Mezon, Direction des Etudes et de Recherches Nouvelles, Centre d'Essais et des Recherches sur les Utilisations du Gaz, Gaz de France, 361 Avenue du President Wilson BP 33, 93211 LaPlaine Saint-Denis Cedex, France
121. J. P. Millhone, CE-13, 5E-080/FORSTAL, U.S. Department of Energy, 1000 Independence Avenue, SW, Washington, DC 20585

122. E. Miura, Heat Pump Technology Center of Japan, Azuma Shurui Bldg., 9-11, Kandaawaji-cho 2-chome, Chiyoda-ku, Tokyo 101, Japan
123. B. Modahl, The Trane Company, 3600 Pammel Creek Road, LaCrosse, WI 54601-7599
124. K. P. Murphy, Allied-Signal, P.O. Box 1087 R, Morristown, NJ 07960
125. G. H. Myers, Gas Research Institute, 8600 West Bryn Mawr Avenue, Chicago, IL 60631
126. Y. Nagaoka, Heat Pump Systems, Gas Utilization Group, Research and Development Institute, 16-25 Shiobaura, 1-chome, Minato-Ku, Tokyo, 105, Japan
127. R. Osborne, Battelle Memorial Institute, Columbus Division, 505 King Ave., Columbus, OH 43201-2693
128. H. Perez-Blanco, 314 Mechanical Engineering Building, Pennsylvania State University, University Park, PA 16802
129. S. Petty, Columbia Gas System Service Corporation, 1600 Dublin Road, P.O. Box 2318, Columbus, OH 43215
130. B. A. Phillips, Phillips Engineering Company, 721 Pleasant Street, St. Joseph, MI 49085
131. B. Plzak, Refrigeration Systems Division, The Trane Company, 3600 Pammel Creek Road, LaCrosse, WI 54601-7599
132. R. Radermacher, University of Maryland, Mechanical Engineering Department, College Park, MD 20742
133. W. Raldow, Swedish National Board for Technical Development, Box 43200, 100 72 Stockholm, Sweden
134. J. Rasson, Lawrence Berkeley Laboratory, 1 Cyclotron Road, Berkeley, CA 94720
135. R. C. Reimann, United Technologies Carrier, 6376 Wavel St., Syracuse, NY 13026
136. C. Ripka, Carrier Corporation, P.O. Box 4808, Carrier Parkway, Syracuse, NY 13221

137. U. Rockenfeller, Rocky Research, 674 Wells Road, Boulder City, NV 89005
138. J. D. Ryan, CE-422, 5H-048/FORSTAL, U.S. Department of Energy, 1000 Independence Avenue, SW, Washington, DC 20585
139. W. A. Ryan, Gas Research Institute, 8600 West Bryn Mawr Avenue, Chicago, IL 60631
140. T. Saito, The University of Tokyo, Department of Mechanical Engineering, 7-3-1 Hongo, Bunkyo, Tokyo 114, Japan
141. U. Schaerer, Swiss Federal Office of Energy, CH-3003 Bern, Switzerland
142. J. Scharfe, Physik Dept. E19, T.U. Muenchen-Garching, D-8046 Muenchen Garching, Federal Republic of Germany
143. P. Scheihing, CE-141, 5G-067/FORSTAL, U.S. Department of Energy, 1000 Independence Avenue, SW, Washington, DC 20585
144. F. Setterwall, The Royal Institute of Technology, Department of Chemical Engineering, S-100 44 Stockholm, Sweden
145. C. T. Sgamboti, United Technology Research Center, 411 Silver Lane, East Hartford, CT 06108
146. S. V. Shelton, Thermax, Inc., 296 14th Street NW, Atlanta, GA 30318
147. J. B. Shrago, Office of Technology Transfer, 405 Kirkland Hall, Vanderbilt University, Nashville, TN 37240
148. K. Snelson, National Research Council Canada, Div. of Mechanical Engineering, Montreal Road, Ottawa, Ontario K1A 0R6, Canada
149. G. F. Sowers, Law Companies Group, Inc., 114 Townpark Dr., Suite 250, Kennesaw, GA 30144-5599
150. H. O. Spauschus, Georgia Institute of Technology, Energy and Materials Sciences Laboratory, Atlanta, GA 30332
151. W. R. Staats, Gas Research Institute, 8600 West Bryn Mawr Avenue, Chicago, IL 60631
152. T. Statt, Electric Power Research Institute, Customer Systems Division, 3412 Hillview Ave., Palo Alto, CA 94303-9743

153. F. Steimle, Institut for Angewandte, Thermodynamik und Klimatechnik, Universitat Essen, Universitat Strasse 15, Postfach 6843, D-4300 Essen 1, Federal Republic of Germany
154. K. Stephan, Institut fur Technische Thermodynamik und Thermische Verfahrenstechnik, Universitat Stuttgart, Pfaffenwaldring 9, FA 1705, Postfach 1140, 7000 Stuttgart 80, Federal Republic of Germany
155. P. Swenson, Consolidated Natural Gas, CNG Tower, Pittsburgh, PA 15222-3199
156. W. E. Tomala, Research, Development & Demonstration, Brooklyn Union Gas, One MetroTech Center, Brooklyn, NY 11201
157. C. Trepp, Eidgenossische Technische Hochschule, Institut fur Verfahrens und Kaltechnik, ETH-Zentrum, 8092, Switzerland
158. T. Uemura, Kansai University, Faculty of Engineering, Senriyama, Suita, Osaka, 564 Japan
159. D. Uselton, Lennox Industries, Inc., P.O. Box 877, Carrollton, TX 75011-0877
160. H. van der Ree, TNO-MT, Laan van Westenenk 501, NL-7334 DT Apeldoorn, The Netherlands
161. G. C. Vliet, Taylor Hall 116, The University of Texas, Austin TX 78712
162. C. M. Walton, College of Engineering, The University of Texas at Austin, Cockrell Hall, Suite 4.2, Austin, TX 78712
163. K. Watanabe, Department of Mechanical Engineering, Keio University, 3-14-1, Hiyoshi, Kohoku-Ku, Yokohama 223, Japan
164. G. Whitacre, Battelle Memorial Institute, Columbus Division, 505 King Ave., Columbus, OH 43201-2693
165. B. D. Wood, College of Engineering and Applied Science, Arizona State University, Tempe, AZ 84281
166. T. Yoshie, Appliance and Installation R&D Dept., Tokyo Gas Co., Ltd., 5-20 Kaigan 1-Chome, Minato-Ku, Tokyo 105, Japan
167. T. Zawacki, Phillips Engineering Company, 721 Pleasant Street, St. Joseph, MI 48095

168. P. Zegers, Commission of the European Communities, Directorate General XII, Wetstraat 200, B-1049 Brussels, Belgium
169. Office of the Assistant Manager for Energy R&D, U.S. Department of Energy, Oak Ridge Operations, Oak Ridge, TN 37831-6269
- 170-171. Office Scientific and Technical Information, P.O. Box 62, Oak Ridge, TN 37831